Title

GEMMA CUP-ASSOCIATED MYB1, an ortholog of axillary meristem regulators, is essential in vegetative reproduction in *Marchantia polymorpha*

Author list and affiliations

Yukiko Yasui,[1,2,#] Shigeyuki Tsukamoto,[1,#] Tomomi Sugaya,[3] Ryuichi Nishihama,[2] Quan Wang,[4] Hirotaka Kato,[1] Katsuyuki T. Yamato,[5] Hidehiro Fukaki,[1] Tetsuro Mimura,[1] Hiroyoshi Kubo,[3] Klaus Theres,[4] Takayuki Kohchi,[2] and Kimitsune Ishizaki[1,6*]

[1]Graduate School of Science, Kobe University, Kobe 657-8501, Japan;

[2]Graduate School of Biostudies, Kyoto University, Kyoto 606-8502, Japan;

[3]Department of Biology, Faculty of Science, Shinshu University, Matsumoto 390-8621, Japan;

[4]Department of Plant Breeding and Genetics, Max Planck Institute for Plant Breeding Research, Carl-von-Linné-Weg 10, D-50829 Cologne, Germany

[5]Faculty of Biology-Oriented Science and Technology, Kindai University, 930 Nishimitani, Kinokawa, Wakayama 649-6493, Japan;

[6]Lead Contact

[*]Corresponding Author:

Kimitsune Ishizaki, Department of Biology, Graduate School of Science, Kobe University, 1-1 Rokkodai, Nada, Kobe 657-8501, Japan

Tel: +81-78-803-5727

E-mail: kimi@emerald.kobe-u.ac.jp

[#]Y.Y. and S.T. contributed equally to this work.

Summary

A variety of plants in diverse taxa can reproduce asexually via vegetative propagation, in which clonal propagules with new meristem(s) are generated directly from vegetative organs. A basal land plant, *Marchantia polymorpha*, develops clonal propagules, gemmae, on the gametophyte thallus from the basal epidermis of a specialized receptacle, the gemma cup. Here we report an R2R3-MYB transcription factor, designated GEMMA CUP-ASSOCIATED MYB 1 (GCAM1), which is an essential regulator of gemma cup development in *M. polymorpha*. Targeted disruption of *GCAM1* conferred a complete loss of gemma cup formation and gemmae generation. Ectopic overexpression of *GCAM1* resulted in formation of cell clumps, suggesting a function of GCAM1 in suppression of cell differentiation. Although gemma cups are a characteristic gametophyte organ for vegetative reproduction in a taxonomically restricted group of liverwort species, phylogenetic and interspecific complementation analyses support the orthologous relationship of GCAM1 to regulatory factors of axillary meristem formation, e.g. Arabidopsis REGULATOR OF AXILLARY MERISTEMS and tomato Blind, in angiosperm sporophytes. The present findings in *M. polymorpha* suggest an ancient acquisition of a transcriptional regulator for production of asexual propagules in the gametophyte, and the use of the regulatory factor for diverse developmental programs, including axillary meristem formation, during land plant evolution.

INTRODUCTION

The plastic nature of plant architecture can be traced back to the activity of meristems, which are pools of pluripotent cells located at the tips of growing plant bodies. In seed plants, the primary shoot apical meristem (SAM) is established during embryonic development. Following germination, secondary meristems are continuously produced in the axils of leaves, and form the basis of branching in flowering plants. Many plant species also develop ectopic meristems at different positions of the plant body [1, 2].

Vegetative reproduction, a form of asexual reproduction in plants, is a developmental process by which clonal progeny arise directly from parental tissues. This process is based on the remarkable potential of plants to proliferate meristems, which develop whole plantlets from differentiated tissues [1, 3, 4]. Diverse plants have the capability for vegetative reproduction, which occurs naturally from a variety of vegetative tissues, e.g. stems (rhizomes:

asparagus, iris, ginger, bulbs: onion, tubers: potato, corms: crocus, and runners: strawberry, wild mint), roots (sweet potato), and leaves (*Kalanchoe*), or can be induced artificially by means of various techniques, including cuttings, grafting, and tissue culture. Vegetative reproduction is considered to be an important strategy for efficient plant propagation and survival in the natural environment [5], as well as for agriculture and horticulture [6].

The liverwort, *Marchantia polymorpha* L., as well as certain related species in the class Marchantiopsida, develops specialized organs for vegetative reproduction, termed the gemma cup or cupule [7]. Clonal propagules, called gemmae, develop from single epidermal cells at the base, or floor, of gemma cups. Thus, the floor cells have the capability to produce clonal plantlets. Gemma cups are formed periodically along the dorsal midrib of a thallus. The restricted occurrence of gemma cups along the midrib suggests that they originate from the dorsal merophyte above the apical cell [7]. Over 100 gemmae can develop in a single gemma cup. The development of gemma cups has been well described on the basis of a series of histological observations on *M. polymorpha* [8]. According to the detailed observations by Barnes and Land [8], the precursors of the floor epidermis in a gemma cup are recognizable as close as the third cell back from the apical cell on the dorsal surface. The floor epidermis is a region where periclinal cell divisions to generate protodermal and subprotodermal cell layers of the air chamber are suppressed, and consecutive elongated epidermal cells are instead observed. The single-layered epidermal cells comprise the gemminiferous region, an area that will become the basal epidermis of a gemma cup. These cells undergo repeated anticlinal divisions to enlarge the area of the gemma cup floor, allowing for increase in gemma production. Some gemma cup floor cells begin to develop gemmae from an early stage of gemma cup development, and growth of the gemma cup occurs concomitantly with gemma development and maturation (Figure S1). The frequency of gemma cup formation is influenced by a variety of environmental factors, such as light and nutrients [9-11]. However, the molecular mechanisms underlying gemma and gemma cup development are largely unknown.

Marchantia polymorpha is a member of an early diverging lineage among land plants. The species offers a number of advantages for genetic studies: low genetic redundancy [12], a haploid-dominant life cycle, and practicable genetic tools, such as high-efficiency transformation and gene modification techniques [13]. Recent molecular genetic studies on bryophytes, including *M. polymorpha*, have revealed several key developmental regulators for

the gametophyte generation that have orthologous counterparts in angiosperms shown to control analogous, but not homologous, developmental processes in the sporophyte generation [14, 15]. These observations suggest that a considerable number of developmental regulatory modules were acquired in the common ancestor of land plants before the divergence of bryophytes and vascular plants.

In the present study, we undertook a comprehensive transcriptome analysis and isolated an R2R3-MYB transcription factor gene, *GCAM1*, which was predominantly upregulated in developing *M. polymorpha* gemma cups. Molecular and genetic characterization revealed a critical role for GCAM1 in gemma cup development. Cell proliferation without tissue differentiation was observed in plants ectopically expressing *GCAM1*. Although the gemma cup is a characteristic gametophytic organ for vegetative reproduction in certain species of Marchantiopsida, phylogenetic and interspecific complementation analyses supported the orthologous relationship of *GCAM1* with angiosperm genes of the R2R3-MYB subfamily 14 [16], which are involved in axillary meristem formation. Potential mechanisms shared between vegetative reproduction in the gametophyte of liverworts and axillary meristem formation in the sporophyte of angiosperms are discussed.

RESULTS

An R2R3-MYB transcription factor is upregulated in the gemma cup

To screen for potential key regulators involved in vegetative reproduction in *M. polymorpha*, we performed RNA-seq analyses comparing the transcriptome of gemma cups with that of the entire young thallus yet to form gemma cups and that of the midrib region (Figure 1A). We obtained more than 14×10^6 reads from each of the samples (triplicates per tissue; Table S1). More than 90% of the reads per library were mapped to the *M. polymorpha* genome sequence version 3.1 [12]. Genes for which the reads per kilobase per million (RPKM) value was > 1 were considered to be 'expressed'. Among the 19,287 annotated genes, 11,699 genes (61%) were expressed in the gemma cup. We identified 1391 and 1483 genes with greater than 2-fold changes in the gemma cup compared with their expression in the young thallus and midrib tissue, respectively. A total of 664 genes were upregulated in both comparisons (Figure 1B and Data S1A–C). Of the 664 genes, 10 were annotated as transcription factors (Table S2).

Among the transcription factors, we focused on Mapoly0034s0034, a gene encoding

an R2R3-MYB transcription factor. The RPKM value of this gene in the gemma cup was 82.1, which represented 100-fold and 13-fold upregulation compared with expression in the young thallus and the midrib, respectively (Table S2). Reverse-transcription quantitative PCR (qRT-PCR) analysis confirmed that Mapoly0034s0034 transcripts accumulated at a significantly higher level in gemma cups than in the young thallus and midrib tissue (Figure 1C). We designated the *Mapoly0034s0034* gene as *GEMMA CUP-ASSOCIATED MYB 1* (*GCAM1*). Genetic nomenclature is as outlined in Bowman *et al*. [17].

Next, we generated transgenic *M. polymorpha* plants expressing a β-glucuronidase (GUS) reporter gene under the control of the *GCAM1* promoter (*GCAM1pro:GUS*). We generated a construct in which the GUS reporter gene was translationally fused to a *GCAM1* genomic fragment, containing 5.2-kb upstream of the ATG start codon. In *GCAM1pro:GUS* transgenic lines, histological GUS staining was detected in the apical notches of the 10-day-old thallus (Figure 2A). In mature thalli with gemma cups, significant promoter activity was detected in the apical notches, the floor of gemma-cups, and developing gemmae (Figure 2B–D).

To analyze the localization of protein accumulation, we inserted the yellow fluorescent protein (Citrine) sequence into the 3′ end of the *GCAM1* coding sequence (CDS) in the *M. polymorpha* genome (Figure S2A and B). The *GCAM1-Citrine* knock-in plants exhibited normal organ development, including gemma cups during vegetative growth (Figure S2C). Consistent with the promoter–reporter analysis, we detected Citrine signals in the nucleus of cells in the developing gemma and gemma-cup floor cells (Figure 2E–M).

GCAM1 is essential for gemma cup formation

To investigate the function of GCAM1, we disrupted *GCAM1* using homologous recombination-mediated gene targeting technology [18]. Two independent *GCAM1* knock-out lines (*gcam1*^{ko}) were isolated from 522 candidates (Figure S2D and E). Reverse transcription PCR (RT-PCR) demonstrated that no transcripts spanning the hygromycin-resistant cassette were detected in the *gcam1*^{ko} plants, whereas truncated *GCAM1* transcripts were detected at a low level (Figure S2F). As the *gcam1*^{ko} plants lack half of the R2R3-MYB DNA-binding domain, we concluded that no functional transcript of *GCAM1* was expressed in *gcam1*^{ko} plants. In the wild-type, 3-week-old thallus developed from a thallus explant containing an apical notch, over ten gemma cups filled with gemmae were observed on the midrib of the

dorsal surface (Figure 3A, C, E). In contrast, no gemma cup development was observed on the dorsal surface of the *gcam1*^{ko} midrib (Figure 3B and D), resulting in no gemma generation. No distinct impairment of thallus growth or development of other vegetative organs, i.e. air chamber, rhizoid, and ventral scales, was observed in *gcam1*^{ko} thalli compared with those of wild-type thalli (Figure 3C–F). We also generated *GCAM1* mutants using CRISPR/Cas9-mediated targeted genome editing [19, 20]. Two independent *GCAM1* mutants for each of two independent target sequences of *GCAM1* exhibited absence of gemma cup development, but no other obvious aberrant phenotype was observed during vegetative growth (Figure S3), and thus the phenotypes were essentially identical to those of *gcam1*^{ko} plants. Altogether, these results demonstrated that *GCAM1* performs a critical role in gemma cup formation.

Generation of gemma cups is correlated with bifurcation (i.e. branching of the apical meristem) of thalli [7]. To clarify whether *GCAM1* may also be involved in branching, we investigated the number of gemma cups and apical notches in the *gcam1*^{ko} line in comparison with those of the wild type. About 20 gemma cups were observed on 3-week-old wild-type thalli, whereas no gemma cups developed in the *gcam1*^{ko} mutants (Figure 3G). In contrast to the conspicuous gemma cup phenotype, *gcam1*^{ko} lines showed periodic bifurcations at a similar frequency to that of the wild type (Figure 3H). Although there were significant differences in the number of apical notches between Tak1 and *gcam1*^{ko} #229 (male), and Tak-2 and *gcam1*^{ko} #181 (female), the trend of differences between the wild type and *gcam1*^{ko} lines were opposite in the sexual background (Figure 3H), which could be caused by polymorphisms in the F_1 population. These results suggest that *GCAM1* does not play a major role in bifurcation of the thallus apical notch.

Overexpression of *GCAM1* promotes proliferation of undifferentiated cells

To further investigate the developmental function of GCAM1, we generated transgenic plants that ectopically overexpressed *GCAM1* under the control of the Mp*ELONGATION FACTOR 1α* regulatory sequence in *M. polymorpha* (Mp*EFpro:GCAM1*). We obtained a significantly lower number of transformants using the Mp*EFpro:GCAM1* construct than usual, and the majority of the obtained Mp*EFpro:GCAM1* lines formed a mass of tiny flat thallus-like structures (Figure S4A–F). Thus, we utilized an inducible system (Figure 4A), in which protein nuclear localization is modulated by a glucocorticoid receptor (GR) domain [21, 22]. In these transgenic plants, GCAM1 function was expected to be induced by treatment with

dexamethasone (DEX). In the wild type, treatment with DEX caused no morphological effect (Figure S4G–L). In the absence of DEX, Mp*EFpro:GCAM1-GR* plants exhibited the wild-type phenotype and formed normal dorsal/ventral organs, i.e. air chambers, gemma cups, scales, and rhizoids (Figure 4B, D, F). Treatment of Mp*EFpro:GCAM1-GR* plants with DEX severely suppressed thallus growth, and cell clumps with no dorsal/ventral organs and few rhizoids were observed (Figure 4C, E, and G). After suspension of the DEX treatment, a number of small thallus branches were generated in random positions (Figure 4H, I and Figure S4M–P). These results implied that GCAM1 functions in the suppression of tissue differentiation and the proliferation of undifferentiated cells that possess the capability to develop into individual thalli when GCAM1 functions are ectopically induced in the gametophyte.

Orthologous relationship of GCAM1 to R2R3-MYBs in subfamily 14

Gemmae and gemma cups are specialized and derived gametophytic organs for vegetative reproduction in certain Marchantiopsida species, a group of complex thalloid liverworts including *M. polymorpha*. However, homologues of *GCAM1* have been identified across diverse branches of land plants. The inferred amino acid sequence of GCAM1 contained an R2R3-MYB DNA-binding domain towards the N-terminus, and showed the highest similarity (3e-59) to REGULATOR OF AXILLARY MERISTEM 3 (RAX3) in a BLASTP search against the *Arabidopsis thaliana* protein database. Our phylogenetic analysis demonstrated that GCAM1 belongs to a clade, the R2R3-MYB subfamily 14, that is clearly separated from the closest subfamilies including the TDF1 group (Figure 5A). It is also noted that GCAM1 and the members in the R2R3-MYB subfamily 14 share a highly conserved exon–intron structure (Figure 5B). Furthermore, relative to other R2R3-MYB proteins, the R2R3-MYB subfamily 14 are characterized by insertion of an additional amino-acid between the first and second conserved Trp residues of the R2 repeat (4^{th} amino acid back from the second conserved Trp residues) [16], and GCAM1 conforms to this rule (Figure 5C). Comprehensive phylogenetic analysis with all R2R3-MYB transcription factors encoded in several genome sequenced plant species including *M. polymorpha* has also supported the orthologous relationship of the Marchantia *GCAM1* (Mp2R-MYB10: Mapoly0034s0034) to the genes in the R2R3-MYB subfamily 14 [12]. These data support strongly the orthologous relationship of GCAM1 to angiosperm proteins in the R2R3-MYB subfamily 14. Some angiosperm

proteins in the R2R3-MYB subfamily 14 are regulatory factors for axillary meristem formation, e.g. *Blind* and *RAX* genes [23-26].

We searched for *GCAM1* homologues in other plant species for which transcriptome data are available in the 1KP project [27]. As mentioned above, *GCAM1* belongs to the R2R3-MYB subfamily 14, which is characterized by an additional amino acid insertion (typically Thr) between the first and second conserved Trp residues of the R2 repeat (Figure 5C, Figure S5E). We located R2R3-MYB genes that have the specific character of subfamily 14 in various liverworts, lycophytes, gymnosperms, and angiosperms, but not in the recently sequenced *Chara braunii* genome [28] nor in the transcriptomes of Zygnematales and Coleochaetales species, which are the extant sister groups of land plants. These data support the emergence of the R2R3-MYB subfamily 14 in the common ancestor of land plants, which diverged at least 430 MYA [29]. However, we did not identify genes of the R2R3-MYB subfamily 14 in the transcriptomic data for mosses and monilophytes, implying secondary loss of the R2R3-MYB subfamily 14 in some branches of bryophytes and ferns.

To examine whether *M. polymorpha GCAM1* is functionally similar to the angiosperm homologues and is able to function in control of axillary meristem formation in angiosperms, we introduced *GCAM1* into the Arabidopsis *rax1 rax2 rax3* triple mutant, which exhibits significant inhibition of axillary bud formation compared with the wild type [24]. Interestingly, expression of *GCAM1* under the control of the Arabidopsis *RAX1* promoter (*RAX1pro:GCAM1*) further inhibited axillary meristem formation in the *rax1 rax2 rax3* triple mutant background (Figure 5D, Figure S5A–D). Given that a non-conserved N-terminal domain is present upstream of (specifically, 28 amino acids from) the R2R3-MYB domain of *GCAM1*, which is absent in angiosperm R2R3-MYB subfamily 14 members (Figure 5B, C), we also tested complementation with a shorter open reading frame (ORF) of *GCAM1* (*GCAM1-s*), which starts from the second start codon in the original *GCAM1* ORF. The *RAX1pro:GCAM1-s* transgenic plants showed notable recovery of axillary meristem formation compared with that of the *rax* triple mutant (Figure 5D, Figure S5A–D). These results demonstrated the capability of *M. polymorpha* GCAM1 to interact with the genetic machinery of axillary meristem formation in the angiosperm *A. thaliana*.

Discussion

Identification of an essential regulator for vegetative reproduction in *M. polymorpha*

The basis of vegetative reproduction in seed plants is the *de novo* meristem formation, which allows development of clonal plants. At present, the molecular mechanism of natural vegetative reproduction is poorly known. In the current study, we identified a key regulator for vegetative reproduction in the basal land plant *M. polymorpha*. Using comprehensive transcriptome analysis and molecular genetic approaches, we identified an R2R3-MYB gene, *GCAM1*, which is an essential factor for gemma cup development in *M. polymorpha*. Loss-of-function mutants of *GCAM1* showed no sign of gemma cup development, but no obvious abnormality was observed in the development of other thallus tissues (Figure 3). This observation suggests that GCAM1 plays a specific role in gemma cup development in the vegetative growth phase of *M. polymorpha*. Our observations on the accumulation of GCAM1 in developing gemma cups and gemmae (Figure 2E–M) corroborated the suggestion of a specific function for *GCAM1* in gemma cup and gemma formation. However, ectopic expression of *GCAM1* did not confer excessive production of gemma cups (Figure 4) and instead suppressed organ differentiation and promoted generation of undifferentiated cell clumps (Figure 4 and Figure S4). After GCAM1 induction was halted at 1 week or 2 weeks after DEX treatment, numerous thalli developed directly from the cell clumps (Figure 4), suggesting that the cell clumps consist of cells with the potential to differentiate into meristematic apical cells of the thallus. These results suggest that GCAM1 might function to suppress tissue differentiation and maintain the undifferentiated status of cells in the gametophyte, which may be essential for the floor cells of the gemma cup to form gemma initials. The role of GCAM1 would be to proliferate floor cells of gemma cups, and to maintain the low differentiation level of these cells, which may be a prerequisite for gemma cup development and gemma initiation. Given that GCAM1 expression was observed not only in the floor cells of the gemma cup, but also in the developing gemmae, GCAM1 may also perform a critical role in gemma differentiation. In gemma development, a gemma initial cell sequentially divides into a flat multicellular body, and two apical meristems are established on opposite sides of the disk [7]. Thus, gemma development can be considered to be a process similar to meristem formation. We surmise that the GCAM1 function to maintain the undifferentiated status of cells would be important for proper gemma development. Alternatively, GCAM1 may have different roles in gemma initiation and gemma differentiation. In stomata differentiation of angiosperms, the bHLH transcription factors SCRM/ICE1 and SCRM2 act throughout the different stages of stomatal development by

changing their interaction partners SPCH, MUTE, and FAMA [30]. Similarly, GCAM1 may interact with different partners to control different sets of genes during gemma differentiation.

The orthologous relationship of *GCAM1* to the regulatory factors for axillary meristem formation in angiosperms

The present phylogenetic analysis indicated that *GCAM1* is orthologous to angiosperm genes in the R2R3-MYB subfamily 14 [16], which includes regulatory factors for axillary meristem formation, e.g. tomato *Blind* and Arabidopsis *RAX* genes [23-26] (Figure 5A). Interspecific complementation analyses demonstrated that *M. polymorpha* GCAM1 can interact with the genetic machinery of axillary meristem formation in Arabidopsis (Figure 5D). These results imply that similar mechanisms control vegetative reproduction in the gametophyte body of the liverwort *M. polymorpha* and axillary meristem formation in the sporophyte body of angiosperms. In Arabidopsis, RAX1 and RAX3 are specifically expressed in the boundary region, axils, between the shoot apical meristem (SAM) and leaf primordia, and regulate axillary meristem formation during vegetative development [24, 25]. In angiosperms, boundary zones are characterized by a lower rate of cell divisions and lower concentrations of auxin and brassinosteroids than those of leaf primordia, resulting in a low degree of differentiation of boundary cells that exhibit higher competence for meristem formation [2, 31]. In Arabidopsis, *CUP-SHAPED COTYLEDON* genes (*CUCs*) are also known to be expressed in boundary zones and required for boundary formation [2]. The tomato gene *Goblet*, which is the tomato orthologue of *CUCs*, promotes shoot formation at the leaflet boundary, suggesting that the specification of the boundary zone is the common basis of axillary bud formation and vegetative reproduction in angiosperms [32]. The cells of the gemma cup floor in the liverwort *M. polymorpha*, in which the ability to regenerate clonal plantlets is maintained, could be considered to show similar characteristics to cells in the boundary zones of angiosperms.

We speculate that such an R2R3-MYB-mediated regulatory mechanism for the establishment and maintenance of cell groups showing a low differentiation level, but retaining the competence to generate meristematic cells, was acquired in the common ancestor of land plants. In the course of land plant evolution, such a regulatory mechanism was co-opted for diverse developmental processes, such as vegetative reproduction in Marchantiales species and axillary bud formation in angiosperms.

Further investigation of the GCAM1-mediated gene regulatory network in *M. polymorpha* and comparison with that for the axillary meristem formation in angiosperms should shed light on the conservation or diversification of regulatory mechanisms for proliferation of meristems in land plants.

ACKNOWLEDGMENTS

The authors thank John L. Bowman and Eduardo Flores-Sandoval (Monash University, Australia) for critical reading of the manuscript; Andrea Busch, Sabine Zachgo (University of Osnabrück, Germany), Shohei Yamaoka, members of T. Kohchi's laboratory for technical assistance and discussions, and Naho Maehara for illustration of graphical abstract. The authors thank Ursula Pfordt and Alexandra Kalde for excellent technical assistance. Research in the Theres laboratory was supported by the Max Planck Society. The RNA-seq analysis was supported by the NIBB Collaborative Research Program 15-823 (K.I.). This study was funded by MEXT KAKENHI grant numbers 18H04836 (R.N.), 25113009 (T.K.), 25119711, 15H01233, 17H06472 (K.I.), and JSPS KAKENHI grant numbers 15H04391, 19H03247 (K.I.) and 19K16167 (Y.Y.), and the SUNTORY Foundation for Life Sciences, the Yamada Science Foundation, and the Asahi Glass Foundation (K.I.). We thank Robert McKenzie, PhD, from Edanz Group (www.edanzediting.com/ac), for editing a draft of this manuscript.

AUTHOR CONTRIBUTIONS

K.I., S.T., and Y.Y. designed the research; S.T., Y.Y., T.S., R.N., Q.W., H.K., K.T., and K.I. performed research; Y.Y., S.T., R.N., Q.W., K.T.Y., H.K., K.T., H.F., T.M., T.K., and K.I. analyzed the data; K.I. and Y.Y. wrote the paper.

DECRALATION OF INTERESTS

The authors declare no competing interests.

FIGURE LEGENDS

Figure 1. Identification of genes preferentially expressed in the gemma cup of *Marchantia polymorpha*

(A) Tissues used for mRNA-seq analysis. GC, gemma cup; TH, 1-week-old thallus; MR, midrib. **(B)** Venn diagram of genes upregulated by more than two-fold in the gemma cup. **(C)** qRT-PCR analysis of Mapoly0034s0034/*GCAM1* in vegetative tissues. The elongation factor 1a (Mp*EF1α*) gene was used as a reference Data are displayed as means ± SD (n = 3), and significant differences with Welch's *t*-test are indicated ($p < 0.01$).
See Figure S1, Table S1, Table S2, and Data S1 for details.

Figure 2 *GCAM1* expression pattern in the vegetative growth stage of *Marchantia polymorpha*

(A–D) Histochemical GUS assay in a representative *GCAM1pro:GUS* line. (A) Ten-day-old thallus. **(B)** Three-week-old thallus with gemma cups. **(C and D)** Transverse sections of developing and mature gemma cups on a 3-week-old thallus. Developing gemma cups are those closely located near the apical notch **(C)** and mature gemma cups are those located in the basal region of the thallus **(D). (E–M)** Accumulation of GCAM1 in the basal floor of the gemma cup. Bright-field **(E–G)**, single confocal **(H–J)**, and merged **(K–M)** images of the basal floor of gemma cups in 17- to 18-day-old thalli in *GCAM1-Citrine* knock-in plants **(E, F, H, I, K, and L)** and the wild type **(G, J, and M).** Dotted lines indicate basal floor cells. Bars, 100 μm **(E–M).** See also Figure S2A–C.

Figure 3. Phenotype of the *gcam1* mutant of *Marchantia polymorpha*

(A and B) Three-week-old thalli grown from tip of thalli of the wild type **(A)** and $gcam1^{ko}$ knock-out mutant **(B).** The thalli were grown from the tip of parental thalli, because gemmae were absent in $gcam1^{ko}$ lines. **(C and D)** Close-up of the tip of thalli of the previous individual, showing gemma cups in the wild type **(C)**, whereas gemma cups were absent in the $gcam1^{ko}$ lines **(D).** Red arrowheads indicate rhizoids. **(E and F)** Transverse sections (5 μm thick) from 3-week-old thalli of the wild type **(E)** and $gcam1^{ko}$ **(F).** Red and blue arrows indicate air chambers and ventral scales, respectively. **(G)** Number of gemma cups in the wild type (WT) and $gcam1^{ko}$ lines. **(H)** Number of apical notches in the wild type and $gcam1^{ko}$ lines. Values are means ± s.d. ($n = 10$), and significant differences detected with Welch's *t*-test are indicated. See also Figure S2D–F and Figure S3.

Figure 4. Induction of GCAM1 function suppresses growth and organ development in thallus of *Marchantia polymorpha*

(A) Schematic representation of the Mp*EFpro:GCAM1-GR* construct. **(B, D, F)** Two-week-old Mp*EFpro:GCAM1-GR* transgenic plant treated with mock. Image of whole thallus (B), and the high-magnification views of the thallus surface by light microscope (D), and scanning electron microscope (F). A number air pores and air chambers are observed in the thallus surface **(D and F)**. **(C, E, and G)**

Two-week-old Mp*EFpro:GCAM1-GR* transgenic plant treated with 10 μM DEX. Image of whole plant (C), and the high-magnification views of the plant by light microscope (E), and scanning electron microscope (G). There is no indication of air chamber development **(E and G)**. Much fewer rhizoids developed from the ventral surface **(E**, inset**)**. **(H)** Two-week-old Mp*EFpro:GCAM1-GR* transgenic plant treated with DEX for the first 7 days and mock for the latter 7 days, and a high-magnification view of the thallus surface (inset). Red arrowhead indicates a developing air chamber. **(I)** Three-week-old Mp*EFpro:GCAM1-GR* transgenic plant treated with DEX for the first 7 days and mock for the latter 14 days, and a high-magnification view of the thallus (inset). Red arrows indicate a set of bifurcated apical notches of thalli. See also Figure S4.

Figure 5. Relationships of GCAM1 and angiosperm R2R3-MYB subfamily 14 orthologues.

(A) Phylogenetic analysis of *GCAM1* and its homologs in plants. Unrooted maximum-likelihood tree generated from the amino acid sequences for the R2R3-MYB DNA-binding domain of GCAM1 and related R2R3-MYB proteins across diverse plant lineages. The numbers at the nodes are bootstrap values calculated from 1000 replicates. The scale bar is evolutionary distance as the rate of amino acid substitutions. *SlBlind* and *CaBlind* are R2R3-MYB genes reported to function in axillary bud formation in *Solanum lycopersicum* and *Capsicum annuum*, respectively. From *A. thaliana*, not only R2R3-MYBs in subfamily 14, but also other R2R3-MYBs in closely related subfamilies were sampled for the phylogenetic analysis. For *Physcomitrella patens* and *Selaginella moellendorffii*, R2R3-MYBs that showed eight highest and two highest similarities to GCAM1, respectively, were sampled. **(B)** Exon–intron structure of *GCAM1*, *AtRAX1*, *AtRAX2*, *AtRAX3*, and *SlBlind*. Box, exon; line, intron; white, 5′ - or 3′ - untranslated region. Red and blue boxes indicate R2R3-MYB domains and the non-conserved N-terminal sequence of 28 a.a. in GCAM1, respectively. **(C)** Multiple alignment of R2R3-MYB domains of GCAM1, AtRAX1, AtRAX2, AtRAX3, and SlBlind. Black asterisks indicate conserved Trp residues in plant R2R3-MYBs, and the blue asterisk indicates a Phe residue conserved in R2R3-MYB subfamily 14 [16]. R2R3-MYBs in subfamily 14 are characterized by an amino-acid insertion compared with other R2R3-MYB subfamilies between the first and the second Trp residues of the R2 repeat, the position of which is indicated by the red triangle. **(D)** Genetic complementation of Arabidopsis *rax1-3 rax2-1 rax3-1* mutant with Arabidopsis *RAX1* and *Marchantia GCAM1* (see Supplementary Figure 5 for details). Lateral shoot formation in rosette leaf axils of the *rax1-3 rax2-1 rax3-1* mutant (*triple rax*, $n = 30$), two independent transformants containing *RAX1*-promoter-driven *RAX1* open reading frame (ORF1) in *rax* triple mutant background (*RAX1pro:RAX1 triple rax*, $n = 15$), two independent transformants containing *RAX1*-promoter-driven *GCAM1* ORF in *rax* triple mutant background (*RAX1pro:GCAM1 triple rax*, $n = 15$), and three independent transgenics containing *RAX1*-promoter-driven shorter version of *GCAM1* ORF in *rax* triple mutant background (*RAX1pro:GCAM1-s triple rax*, $n = 15$). Values represent means ± SE.

Asterisks indicate significant differences relative to the triple *rax* mutant (Student's t-test, *$p < 0.05$, **$p < 0.02$, ***$p < 0.0001$). See also Figure S5.

STAR METHODS

LEAD CONTACT AND MATERIALS AVAILABILITY

Further information and requests for resources and reagents should be directed to and will be fulfilled by the Lead Contact, Kimitsune Ishizaki (kimi@emerald.kobe-u.ac.jp). Please note that the transfer of transgenic plants will be subject to MTA and any relevant import permits.

KEY RESOURCE TABLE

(Attached)

EXPERIMENTAL MODEL AND SUBJECT DETAILS

Plant material and growth conditions

Male and female accessions of *M. polymorpha*, Takaragaike-1 (Tak-1) and Takaragaike-2 (Tak-2), respectively [33], were maintained asexually. F_1 spores generated by crossing Tak-2 and Tak-1 were used for generation of *gcam1*^{ko} and *GCAM1-Citrine* knock-in plants. Formation of sexual organs was induced by far-red irradiation as described previously[34]. Mature sporangia were collected 3–4 weeks after crossing, air-dried for 7–10 days, and stored at −80°C until use.

Marchantia polymorpha plants were cultured using half-strength Gamborg's B5 medium [35] containing 1% agar under 50–60 μmol photons m^{-2} s^{-1} continuous white light with a cold cathode fluorescent lamp (OPT-40C-N-L; Optrom, Miyagi, Japan) or light-emitting diode (VGL-1200W; SYNERGYTEC, Tokushima, Japan) at 22°C unless otherwise defined.

METHOD DETAILS

RNA extraction and Illumina sequencing

Developing gemma cups located within 3 mm from an apical notch of 3-week-old thalli were manually dissected and immediately immersed in RNAlater (Thermo Fisher Scientific, Waltham, MA, USA). For the control, the midrib region between gemma cups of 3-week-old thalli and 1-week-old thalli, which had no visible gemma cups, were also sampled. The collected samples were divided into three pools for extraction of total RNA.

Total RNA was extracted with the RNeasy® Plant Mini Kit (QIAGEN) in accordance with the manufacturer's protocol. The quality and quantity of resultant total RNA were evaluated using a NanoDrop™ 1000 spectrophotometer (Thermo Fisher Scientific), Qubit® 2.0 Fluorometer (Thermo Fisher Scientific), and a Bioanalyzer RNA6000 Nano Kit (Agilent Technologies, Santa Clara, CA, USA). The sequence libraries were constructed with a TruSeq™ RNA Sample Prep Kit v2 (Illumina, San Diego, CA, USA) in accordance with the manufacturer's protocol. The quality and quantity of each library were determined using a Bioanalyzer with High Sensitivity DNA kit (Agilent Technologies), and KAPA Library Quantification Kit for Illumina (Nippon Genetics). Equal amounts of each library were mixed to make the 2 nM pooled library. Illumina sequencing was performed using a HiSeq 2000 platform (Illumina) to produce 101 single-end data. All reads obtained have been deposited in the DDBJ and are available through the Sequence Read Archive (SRA) under the accession number DRA005912.

RNA-seq data analysis

The resultant reads were mapped to the draft genome of *M. polymorpha* version 3.1 by TopHat ver 2.1.1 [36] with the default parameters. To identify differentially expressed genes (DEGs), the mapped reads from different samples were compared by Cuffdiff 2.2.1 [37] using the default parameters and transcript annotation generated on the Marchantia genome assembly ver. 3.1 [12]. Among DEGs, genes with a log2-fold change >1 were considered as preferentially expressed in the gemma cup (for details, see details in Data S1A-C). The supercomputers of the Academic Center for Computing and Media Studies at Kyoto University and of the Computing Center at the Faculty of Biology-Oriented Science and Technology, Kindai University were used for computation.

Quantitative RT-PCR analysis

One microgram of total RNA was reverse-transcribed in a 20 µl reaction mixture using ReverTra Ace® qPCR RT Master Mix with gDNA remover (TOYOBO). After the reaction, the cDNA samples were diluted with 220 µl distilled water and 2 µl aliquots were amplified with the LightCycler® Nano Real-time PCR Detection System (Roche Applied Science, Tokyo, Japan) using the KOD SYBR® qRT-PCR Mix (TOYOBO). The PCR cycling program was performed in accordance with the manufacturer's protocol. The primers used in these

experiments are listed in Table S3. Mp*EF1α* was used as an internal control.

Generation of transformants for promoter–reporter analysis

To construct *GCAM1pro:GUS*, the *GCAM1* genomic region, including a 5593-bp fragment upstream of the 83rd Arg codon in the second exon, was amplified from Tak-1 genomic DNA by PCR with the primers GCAM1pro_L1 and GCAM1pro_R2 and cloned into the pENTR™/D-TOPO® cloning vector (Life Technologies, Rockville, MD, USA). This entry vector was used in the Gateway® LR reaction (Life Technologies) with the Gateway binary vector pMpGWB104 [38] to generate the *GCAM1pro:GUS* binary construct, in which the *GUS* reporter gene was translationally fused at the middle of the second exon of *GCAM1*. The *GCAM1pro:GUS* vectors were introduced into regenerating thalli of Tak-1 by *Agrobacterium*-mediated transformation as previously described [39]. Transformants were selected with 10 μg/ml hygromycin B and 100 μg/ml cefotaxime.

Generation of *gcam1^{ko}* and *GCAM1-Citrine* knock-in plants

For knock-in and knock-out experiments, Tak-1 genomic sequences were amplified by PCR with KOD FX Neo DNA polymerase (TOYOBO) and the primer pair listed in Table S3. The amplified products were inserted into the *Pac*I and *Asc*I sites of pJHY-TMp1 [18] and pJHY-TMp1-Cit[40] to generate *gcam1^{ko}* and *GCAM1-Citrine* transformants, respectively. The vectors were introduced into germinating spores via *Agrobacterium tumefaciens* GV2260 as described previously[18]. Transformants were selected with 10 μg/ml hygromycin B and 100 μg/ml cefotaxime. The transformants harboring the targeted insertions were selected by PCR with KOD FX Neo DNA polymerase and the primer pairs listed in Table S3 and Figure S2.

CRISPR/Cas9-based genome editing of *GCAM1*

Loss-of-function mutants of *GCAM1* were generated with the CRISPR/Cas9 system as described previously [20, 41]. We selected two target sequences, one located in the first exon, and the other located in the second exon of *GCAM1* (Figure S4). An off-target search was performed using casOT[42]. Synthetic oligo DNAs for respective target sites shown in Table S3 were annealed, inserted into the entry vector pMpGE_En01, and then introduced into the destination vector pMpGE011 [20, 41]. The vectors were introduced into regenerating thalli of Tak-1 via *A. tumefaciens* GV2260 [39], and transformants were selected with 0.5 μM

chlorsulfuron. Genomic DNA was isolated from transformants and amplified from the target region by PCR. The PCR product was used for sequencing of the respective target sites with an ABI 3100 genetic analyzer (Applied Biosystems, Foster City, CA, USA).

Visualization of GCAM1-Citrine

Transverse sections of *GCAM1-Citrine* knock-in thalli with apical notches were generated with a pair of razors, and observed under a confocal laser scanning microscope (Olympus FLUOVIEW FV1000, Tokyo, Japan). Excitation and emission wavelengths for Citrine fluorescence were 515 nm (Ar laser) and 520–570 nm, respectively.

Histology and light microscopy

For histochemical GUS staining, *GCAM1pro:GUS* plants were grown on half-strength B5 medium for respective periods under continuous white light. GUS staining was performed as described previously and at least five independent lines were observed for GUS staining patterns using S8APO (Leica Microsystems) and DMS1000 (Leica) stereoscopic microscopes, or an upright light microscope Axio Scope.A1 (Zeiss) equipped with an AxioCam ERc5c camera (Zeiss).

For plastic-embedded sectioning, 3-week-old thalli developed from gemmae were dissected into small pieces and transferred to fixative solution (2% glutaraldehyde in 0.05 M phosphate buffer, pH 7.0), evacuated with a water aspirator until the specimens sank, and fixed for 2 days at room temperature. The samples were dehydrated in a graded ethanol series and embedded in Technovit 7100 plastic resin. Semi-thin sections (5 μm thickness) for light microscopy were obtained with a microtome (HM 335E, Leica Microsystems, Heerbrugg, Switzerland) and stained with toluidine blue O.

For scanning electron microscopy, plant samples were frozen in liquid nitrogen and directly observed on a VHX-D500 microscope (KEYENCE, Osaka, Japan).

Generation of *GCAM1*-overexpressing plants

To generate Mp*EFpro:GCAM1*, the *GCAM1* coding sequence was amplified by PCR using KOD Plus Neo DNA polymerase (TOYOBO) with the primer set GCAM1-cds-L1/GCAM1-cds-sR and cloned into the pENTR/D-TOPO cloning vector. The entry vector was used in the Gateway LR reaction with the Gateway binary vector pMpGWB103 [38]. The

MpEFpro:GCAM1 vector was introduced into regenerating thalli of Tak-1 as previously described [39]. Transformants were selected with 10 μg/ml hygromycin B and 100 μg/ml cefotaxime.

To construct Mp*EFpro:GCAM1-GR*, the *GCAM1* CDS was amplified by PCR using KOD Plus Neo DNA polymerase (TOYOBO) with the primer set GCAM1-cds-L1/GCAM1-cds-nsR and cloned into the pENTR/D-TOPO cloning vector. The entry vector was used in the Gateway LR reaction with the Gateway binary vector pMpGWB313 [38]. The Mp*EFpro:GCAM1-GR* vector was introduced into regenerating thalli of Tak-1 as previously described [39]. Transformants were selected with 0.5 μM chlorsulfuron and 100 μg/ml cefotaxime.

The transformants and mutants were named consistent with the nomenclatural rules for *M. polymorpha* [17].

Phenotypic analysis of Mp*EFpro:GCAM1-GR* plants

In the vegetative phase, DEX treatment of *MpEFpro:GCAM1-GR* plants was performed by culture in half-strength Gamborg's B5 medium containing 10 μM DEX or applying 200 μL of 10 μM DEX solution to plants.

Phylogenetic analysis of GCAM1

For phylogenetic analysis of GCAM1 and related homologous R2R3-MYBs, sequence information was obtained from the PlantTFDB [43] and Phytozome databases. A multiple alignment of amino acid sequences of GCAM1 and homologous R2R3-MYBs was first constructed using COBALT [44] and then using the MUSCLE program [45] implemented in SeaView version 4.5.4 [46] with the default parameters. The alignment is available as Data S2. The conserved region covering the R2R3-MYB domain was extracted before phylogenetic tree construction, which was performed using the maximum likelihood method with PhyML [47] with the LG substitution model. A bootstrap analysis with 1000 replicates was performed in each analysis to assess statistical support for the topology. The phylogenetic tree was visualized using FigTree (http://tree.bio.ed.ac.uk/software/figtree/).

Multiple alignment of GCAM1 and related homologues in diverse land plants

Homologues of GCAM1 were searched and obtained from Phytozome databases, *Picea abies*

genome [48], and transcriptome data generated by 1000 Plant (1KP) project [27]. A multiple alignment of amino acid sequences of GCAM1 and homologous R2R3-MYBs was constructed using the MUSCLE program [45].

Introduction of *GCAM1* into an Arabidopsis *rax* triple mutant

To generate a RAX1 promoter construct, the upstream region of Arabidopsis *RAX1* including the promoter and 5′ untranslated region (2939 bp) were amplified by PCR using the primers Myb37-pro-SbfIF and Myb37-pro-AscIR. The resulting PCR fragment was inserted into the *Sbf*I and *Asc*I sites of the pGPTV-BAR-AscI vector [49] in front of the *GUS* gene (Vector pFY124). A GFP fragment was amplified using the primers GFPAscIF and GFPpolylinkerR. This PCR fragment was introduced into the *Asc*I and *Sac*I sites of pFY124 introducing a new *Avr*II site for the following constructions (Vector pQW154).

The *RAX1* open reading frame was amplified by PCR using the primers RAX1AscIF and RAX1SacIR. The PCR fragment was inserted into the *Asc*I and *Sac*I sites of pQW154. The GCAM1 open reading frame was amplified using the primers GCAM1AscIF and GCAM1AvrIIR. The PCR fragment was inserted into the *Asc*I and *Avr*II sites of pQW154. The ORF from the second methionine codon of the GCAM1 coding sequence (GCAM1-s; from +85 to the stop codon) was amplified using the primers GCAM1New AscIF and GCAM1AvrIIR. The PCR fragment was inserted into the *Asc*I and *Avr*II sites of pQW154.

The *RAX1pro:RAX1*, *RAX1pro:GCAM1*, and *RAX1pro:GCAM1-s* constructs were introduced into the Arabidopsis *rax1-3 rax2-1 rax3-1* mutant [24] using the floral dip method, and T_3 homozygous transgenic lines were used for further analysis.

For cultivation under short-day conditions, Arabidopsis plants were grown in a controlled environment room under a 8 h/16 h (light/dark) photoperiod, 20ºC/18ºC (day/night) temperatures, and 50% relative humidity. Flowering was induced after 4 weeks by transferring the plants to a 16 h/8 h (light/dark) photoperiod. Cultivation under long-day conditions was done in a controlled greenhouse with additional artificial light when needed.

Axillary bud formation was analyzed after the onset of flowering using a stereomicroscope as previously described [50]. Buds that had produced one or two leaf primordia as well as elongating lateral shoots were scored as leaf axils that had established axillary meristems.

QUANTIFICATION AND STATISTICAL ANALYSIS

We used Welchi's t-test or student's t-test to evaluate statistical significance as shown in the legends for Figures 1, 3, and 5. Experimental sample sizes and statistical methods detail are given in the legends for Figures 1, 3, and 5. The row data of axillary bud formation for Figure 5H is provided in Figure S5.

DATA AND CODE AVAILABILITY

All reads obtained have been deposited in the DDBJ and are available through the Sequence Read Archive (SRA) under the accession number DRA005912. The authors declare that all data supporting the findings of this study are available within the manuscript and its supplementary files or are from the corresponding author upon request.

SUPPLEMENTAL DATA FILES

Data S1. List of genes upregulated in the gemma cup. Related to Figure 1B and STAR Methods.

A) List of 1391 genes upregulated by >2 times in the gemma cup in comparison with the young thallus (GC vs TH in Figure 1B). B) List of 1483 genes upregulated by >2 times in the gemma cup in comparison with the midrib (GC vs MR in Figure 1B). C) List of 664 genes upregulated by >2 times in the gemma cup in comparison with the young thallus and midrib (overlap of GC vs TH and GC vs MR in Figure 1B)

Data S2. Multiple alignment of GCAM1 and related R2R3-MYBs used for phylogenetic analysis. Related to Figure 5A and STAR Methods.

REFERENCES

1. Steeves, T.A., and Sussex, I.M. (1989). Patterns in plant development, 2 Edition, (Cambridge: Cambridge University Press).
2. Wang, Q., Hasson, A., Rossmann, S., and Theres, K. (2016). Divide et impera: boundaries shape the plant body and initiate new meristems. New Phytol. *209*, 485-498.
3. Steward, F.C., Mapes, M.O., Kent, A.E., and Holsten, R.D. (1964). Growth and development of cultured plant cells. Science *143*, 20-27.
4. Steward, F.C., Mapes, M.O., and Mears, K. (1958). Growth and organized development of cultured cells. II. Organization in cultures grown from freely suspended cells. Am. J. Bot. *45*, 705-708.
5. Klimesˇová, J., and Klimeš, L. (2007). Bud banks and their role in vegetative regeneration – A literature review and proposal for simple classification and assessment. Perspect. Plant Ecol. Evol. Syst. *8*, 115-129.
6. Davis, F.T., Geneve, R.L., Wilson, S.E., Hartmann, H.T., Kester, D.E. (2017). Hartmann & Kester's Plant Propagation: Principles and Practices, (Pearson).
7. Shimamura, M. (2016). *Marchantia polymorpha*: Taxonomy, phylogeny and morphology of a model system. Plant Cell Physiol. *57*, 230-256.
8. Barnes, C.R., and Land, W.J.G. (1908). Bryological papers. II. The origin of the cupule of Marchantia. Bot. Gaz. *46*, 401-409.
9. Voth, P.D., and Hamner, K.C. (1940). Responses of *Marchantia polymorpha* to nutrient dupply and p dhotoperiod. Bot. Gaz. *102*, 169-205.
10. Voth, P.D. (1941). Gemmae-cup production in *Marchantia polymorpha* and its response to calcium deficiency and supply of other nutrients. Bot. Gaz. *103*, 310-325.
11. Benson-Evans, K. (1964). Physiology of the reproduction of bryophytes. The Bryologist *67*, 431-445.
12. Bowman, J.L., Kohchi, T., Yamato, K.T., Jenkins, J., Shu, S., Ishizaki, K., Yamaoka, S., Nishihama, R., Nakamura, Y., Berger, F., et al. (2017). Insights into land plant evolution garnered from the *Marchantia polymorpha* genome. Cell *171*, 287-304 e215.
13. Ishizaki, K., Nishihama, R., Yamato, K.T., and Kohchi, T. (2016). Molecular genetic tools and techniques for *Marchantia polymorpha* research. Plant Cell Physiol. *57*, 262-270.
14. Ishizaki, K. (2017). Evolution of land plants: insights from molecular studies on basal lineages. Biosci. Biotechnol. Biochem. *81*, 73-80.
15. Pires, N.D., and Dolan, L. (2012). Morphological evolution in land plants: new designs with old genes. Philos. Trans. R. Soc. Lond. B Biol. Sci. *367*, 508-518.
16. Stracke, R., Werber, M., and Weisshaar, B. (2001). The R2R3-MYB gene family in *Arabidopsis thaliana*. Curr. Opin. Plant Biol. *4*, 447-456.
17. Bowman, J.L., Araki, T., Arteaga-Vazquez, M.A., Berger, F., Dolan, L., Haseloff, J., Ishizaki, K., Kyozuka, J., Lin, S.-S., Nagasaki, H., et al. (2016). The naming of names: Guidelines for gene nomenclature in Marchantia. Plant Cell Physiol. *57*, 257-261.
18. Ishizaki, K., Johzuka-Hisatomi, Y., Ishida, S., Iida, S., and Kohchi, T. (2013). Homologous recombination-mediated gene targeting in the liverwort *Marchantia*

polymorpha L. Sci. Rep. *3*, 1532.

19. Sugano, S.S., Shirakawa, M., Takagi, J., Matsuda, Y., Shimada, T., Hara-Nishimura, I., and Kohchi, T. (2014). CRISPR/Cas9-mediated targeted mutagenesis in the liverwort *Marchantia polymorpha* L. Plant Cell Physiol. *55*, 475-481.
20. Sugano, S.S., Nishihama, R., Shirakawa, M., Takagi, J., Matsuda, Y., Ishida, S., Shimada, T., Hara-Nishimura, I., Osakabe, K., and Kohchi, T. (2018). Efficient CRISPR/Cas9-based genome editing and its application to conditional genetic analysis in *Marchantia polymorpha*. PLoS One *13*, e0205117.
21. Lloyd, A.M., Schena, M., Walbot, V., and Davis, R.W. (1994). Epidermal cell fate determination in Arabidopsis: patterns defined by a steroid-inducible regulator. Science *266*, 436-439.
22. Schena, M., Lloyd, A.M., and Davis, R.W. (1991). A steroid-inducible gene expression system for plant cells. Proc. Natl. Acad. Sci. U. S. A. *88*, 10421-10425.
23. Schmitz, G., Tillmann, E., Carriero, F., Fiore, C., Cellini, F., and Theres, K. (2002). The tomato Blind gene encodes a MYB transcription factor that controls the formation of lateral meristems. Proc. Natl. Acad. Sci. U. S. A. *99*, 1064-1069.
24. Müller, D., Schmitz, G., and Theres, K. (2006). Blind homologous R2R3 Myb genes control the pattern of lateral meristem initiation in Arabidopsis. Plant Cell *18*, 586-597.
25. Keller, T., Abbott, J., Moritz, T., and Doerner, P. (2006). Arabidopsis REGULATOR OF AXILLARY MERISTEMS1 controls a leaf axil stem cell niche and modulates vegetative development. Plant Cell *18*, 598-611.
26. Jeifetz, D., David-Schwartz, R., Borovsky, Y., and Paran, I. (2011). CaBLIND regulates axillary meristem initiation and transition to flowering in pepper. Planta *234*, 1227-1236.
27. Matasci, N., Hung, L.H., Yan, Z., Carpenter, E.J., Wickett, N.J., Mirarab, S., Nguyen, N., Warnow, T., Ayyampalayam, S., Barker, M., et al. (2014). Data access for the 1,000 Plants (1KP) project. Gigascience *3*, 17.
28. Nishiyama, T., Sakayama, H., de Vries, J., Buschmann, H., Saint-Marcoux, D., Ullrich, K.K., Haas, F.B., Vanderstraeten, L., Becker, D., Lang, D., et al. (2018). The Chara genome: Secondary complexity and implications for plant terrestrialization. Cell *174*, 448-464 e424.
29. Morris, J.L., Puttick, M.N., Clark, J.W., Edwards, D., Kenrick, P., Pressel, S., Wellman, C.H., Yang, Z., Schneider, H., and Donoghue, P.C.J. (2018). The timescale of early land plant evolution. Proc. Natl. Acad. Sci. U. S. A. *115*, E2274-E2283.
30. Kanaoka, M.M., Pillitteri, L.J., Fujii, H., Yoshida, Y., Bogenschutz, N.L., Takabayashi, J., Zhu, J.K., and Torii, K.U. (2008). SCREAM/ICE1 and SCREAM2 specify three cell-state transitional steps leading to arabidopsis stomatal differentiation. Plant Cell *20*, 1775-1785.
31. Wang, Q., Kohlen, W., Rossmann, S., Vernoux, T., and Theres, K. (2014). Auxin depletion from the leaf axil conditions competence for axillary meristem formation in Arabidopsis and tomato. Plant Cell *26*, 2068-2079.
32. Rossmann, S., Kohlen, W., Hasson, A., and Theres, K. (2015). Lateral suppressor and Goblet act in hierarchical order to regulate ectopic meristem formation at the base of tomato leaflets. Plant J. *81*, 837-848.

33. Ishizaki, K., Chiyoda, S., Yamato, K.T., and Kohchi, T. (2008). *Agrobacterium*-mediated transformation of the haploid liverwort *Marchantia polymorpha* L., an emerging model for plant biology. Plant Cell Physiol. *49*, 1084-1091.
34. Chiyoda, S., Ishizaki, K., Kataoka, H., Yamato, K.T., and Kohchi, T. (2008). Direct transformation of the liverwort *Marchantia polymorpha* L. by particle bombardment using immature thalli developing from spores. Plant Cell Rep. *27*, 1467-1473.
35. Gamborg, O.L., Miller, R.A., and Ojima, K. (1968). Nutrient requirements of suspension cultures of soybean root cells. Exp. Cell Res. *50*, 151-158.
36. Kim, D., Pertea, G., Trapnell, C., Pimentel, H., Kelley, R., and Salzberg, S.L. (2013). TopHat2: accurate alignment of transcriptomes in the presence of insertions, deletions and gene fusions. Genome Biol. *14*, R36.
37. Trapnell, C., Roberts, A., Goff, L., Pertea, G., Kim, D., Kelley, D.R., Pimentel, H., Salzberg, S.L., Rinn, J.L., and Pachter, L. (2012). Differential gene and transcript expression analysis of RNA-seq experiments with TopHat and Cufflinks. Nat. Protoc. *7*, 562-578.
38. Ishizaki, K., Nishihama, R., Ueda, M., Inoue, K., Ishida, S., Nishimura, Y., Shikanai, T., and Kohchi, T. (2015). Development of Gateway binary vector series with four different selection markers for the liverwort *Marchantia polymorpha*. PLoS One *10*, e0138876.
39. Kubota, A., Ishizaki, K., Hosaka, M., and Kohchi, T. (2013). Efficient *Agrobacterium*-mediated transformation of the liverwort *Marchantia polymorpha* using regenerating thalli. Biosci. Biotechnol. Biochem. *77*, 167-172.
40. Yamaoka, S., Nishihama, R., Yoshitake, Y., Ishida, S., Inoue, K., Saito, M., Okahashi, K., Bao, H., Nishida, H., Yamaguchi, K., et al. (2018). Generative cell specification requires transcription factors evolutionarily conserved in land plants. Curr. Biol. *28*, 479-486 e475.
41. Sugano, S.S., and Nishihama, R. (2018). CRISPR/Cas9-based genome editing of transcription factor genes in *Marchantia polymorpha*. Methods Mol. Biol. *1830*, 109-126.
42. Xiao, A., Cheng, Z., Kong, L., Zhu, Z., Lin, S., Gao, G., and Zhang, B. (2014). CasOT: a genome-wide Cas9/gRNA off-target searching tool. Bioinformatics *30*, 1180-1182.
43. Jin, J., Tian, F., Yang, D.C., Meng, Y.Q., Kong, L., Luo, J., and Gao, G. (2017). PlantTFDB 4.0: toward a central hub for transcription factors and regulatory interactions in plants. Nucleic Acids Res. *45*, D1040-D1045.
44. Papadopoulos, J.S., and Agarwala, R. (2007). COBALT: constraint-based alignment tool for multiple protein sequences. Bioinformatics *23*, 1073-1079.
45. Edgar, R.C. (2004). MUSCLE: multiple sequence alignment with high accuracy and high throughput. Nucleic Acids Res. *32*, 1792-1797.
46. Gouy, M., Guindon, S., and Gascuel, O. (2010). SeaView version 4: A multiplatform graphical user interface for sequence alignment and phylogenetic tree building. Mol. Biol. Evol. *27*, 221-224.
47. Guindon, S., Dufayard, J.F., Lefort, V., Anisimova, M., Hordijk, W., and Gascuel, O. (2010). New algorithms and methods to estimate maximum-likelihood phylogenies: assessing the performance of PhyML 3.0. Syst. Biol. *59*, 307-321.

48. Nystedt, B., Street, N.R., Wetterbom, A., Zuccolo, A., Lin, Y.C., Scofield, D.G., Vezzi, F., Delhomme, N., Giacomello, S., Alexeyenko, A., et al. (2013). The Norway spruce genome sequence and conifer genome evolution. Nature *497*, 579-584.
49. Überlacker, B., and Werr, W. (1996). Vectors with rare-cutter restriction enzyme sites for expression of open reading frames in transgenic plants. Mol. Breed. *2*, 293-295.
50. Raman, S., Greb, T., Peaucelle, A., Blein, T., Laufs, P., and Theres, K. (2008). Interplay of miR164, CUP-SHAPED COTYLEDON genes and LATERAL SUPPRESSOR controls axillary meristem formation in *Arabidopsis thaliana*. Plant J. *55*, 65-76.

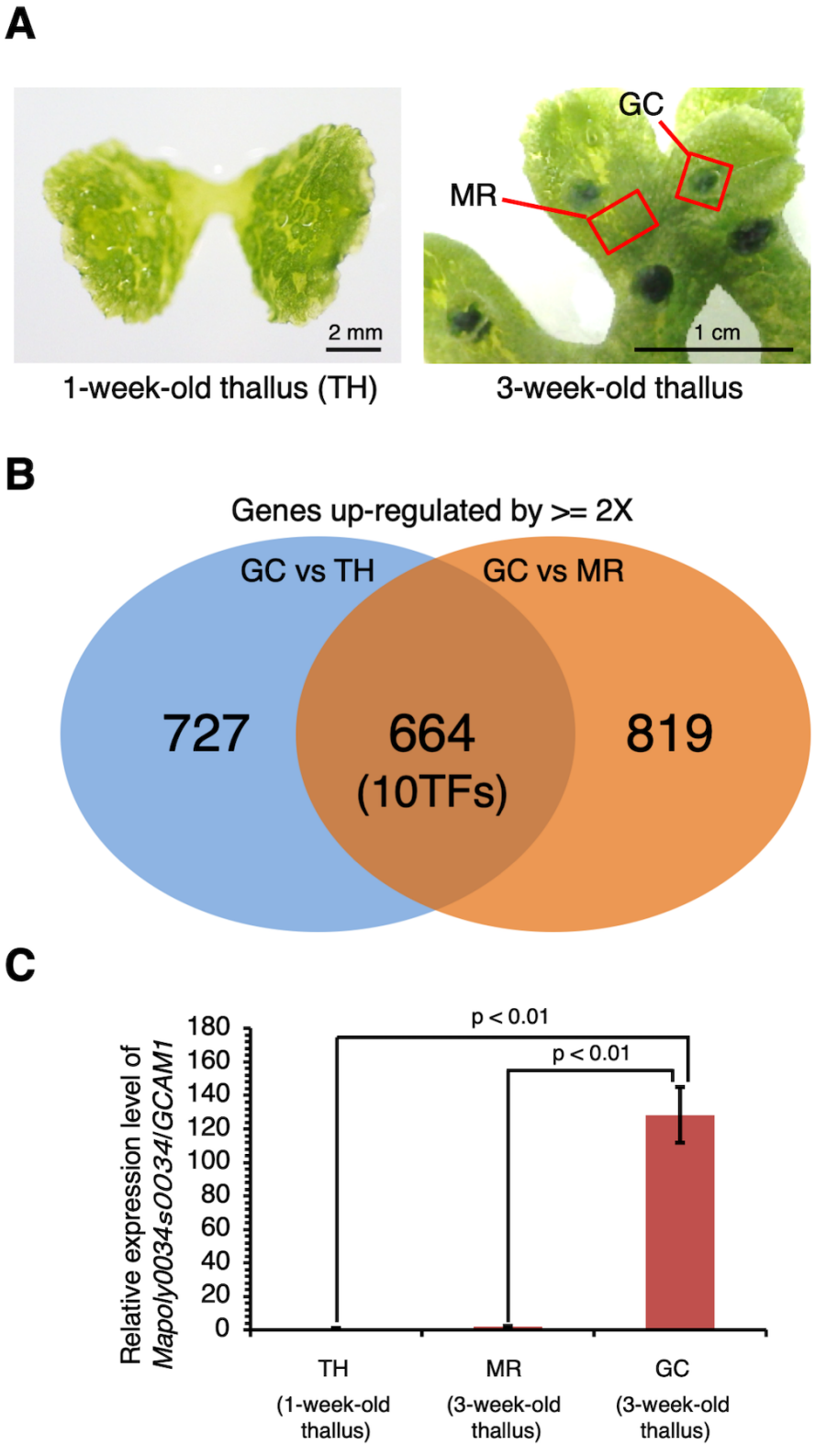

Figure 1. Yasui et al.

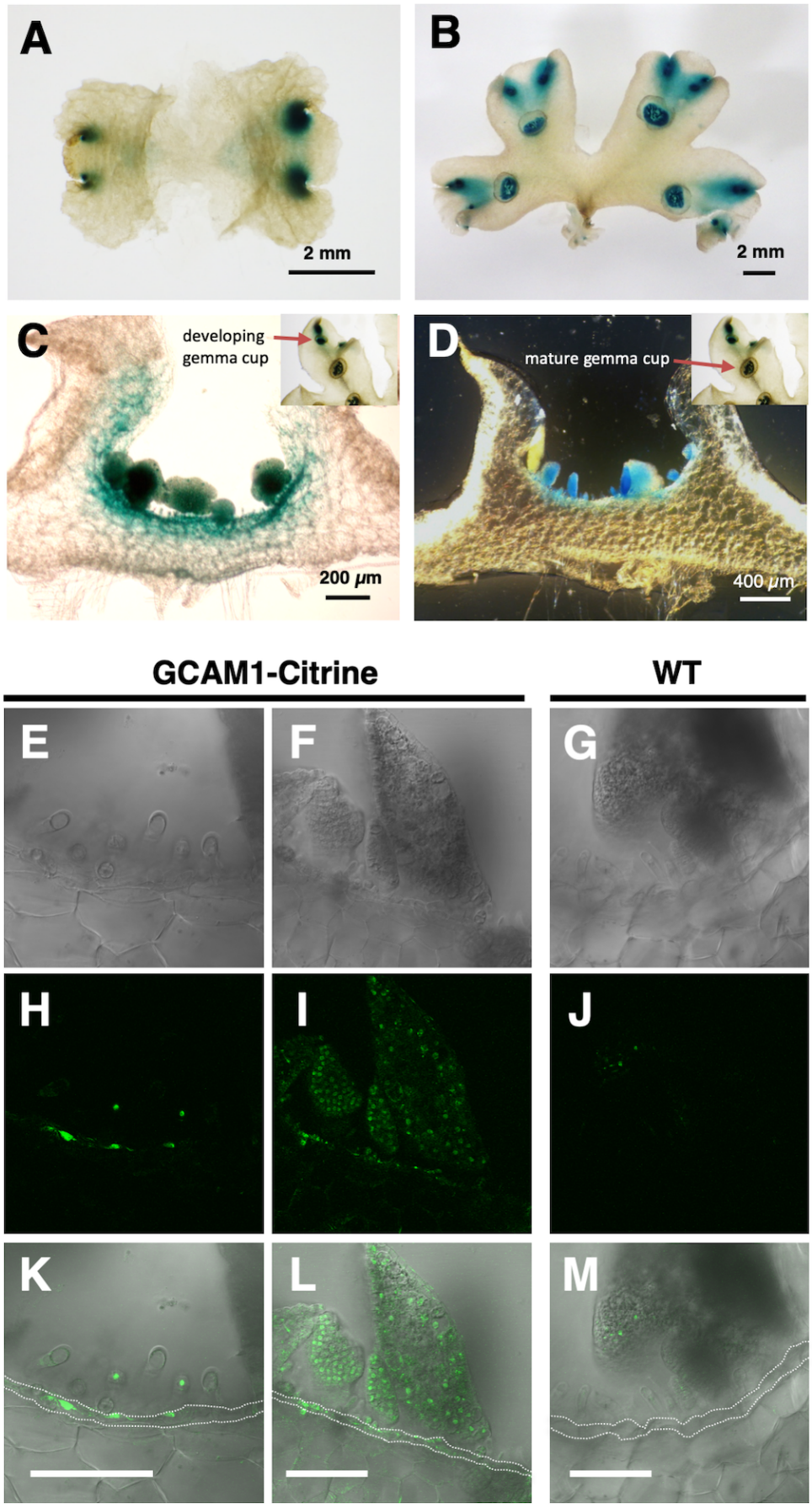

Figure 2. Yasui et al.

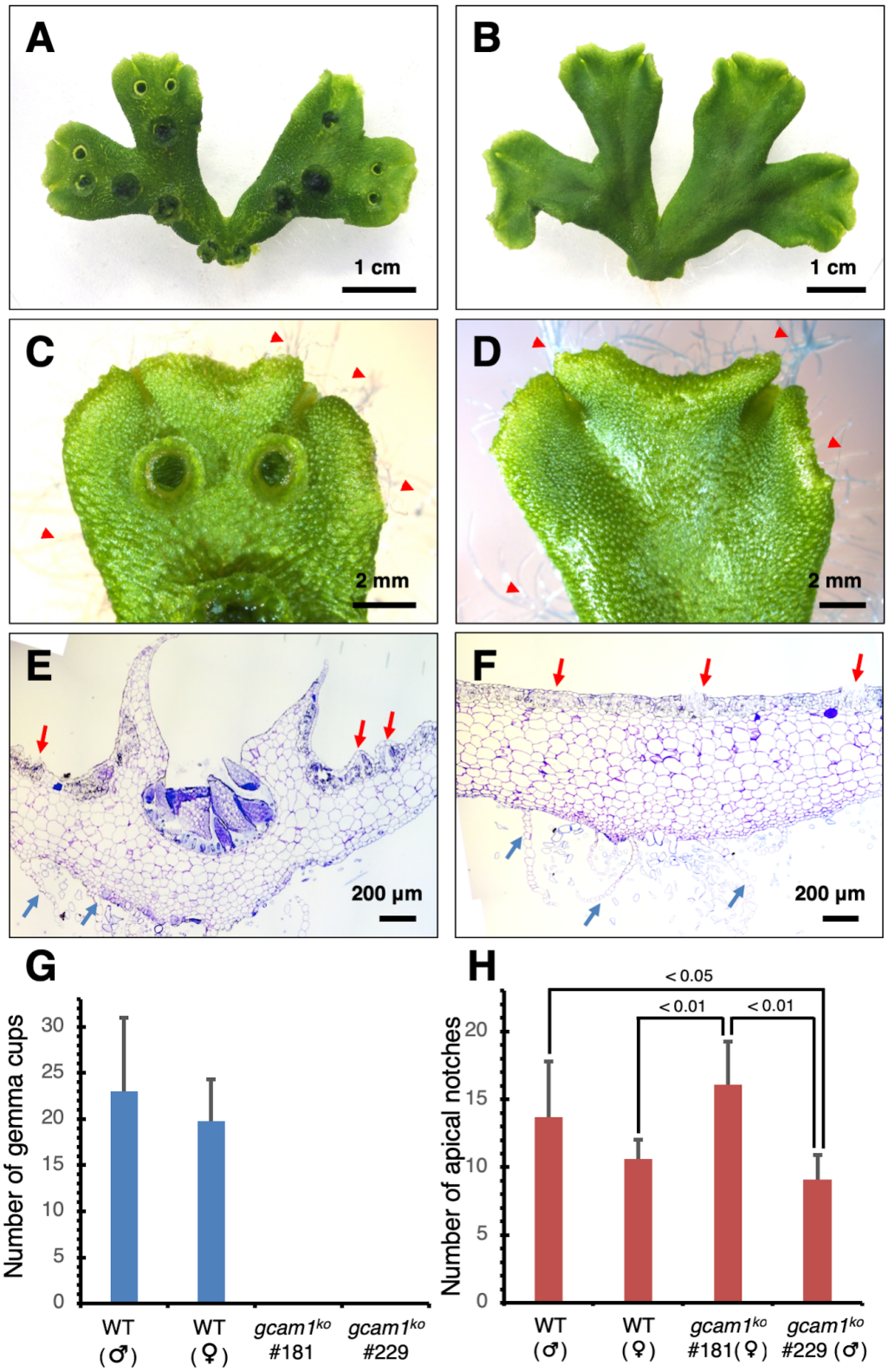

Figure 3. Yasui et al.

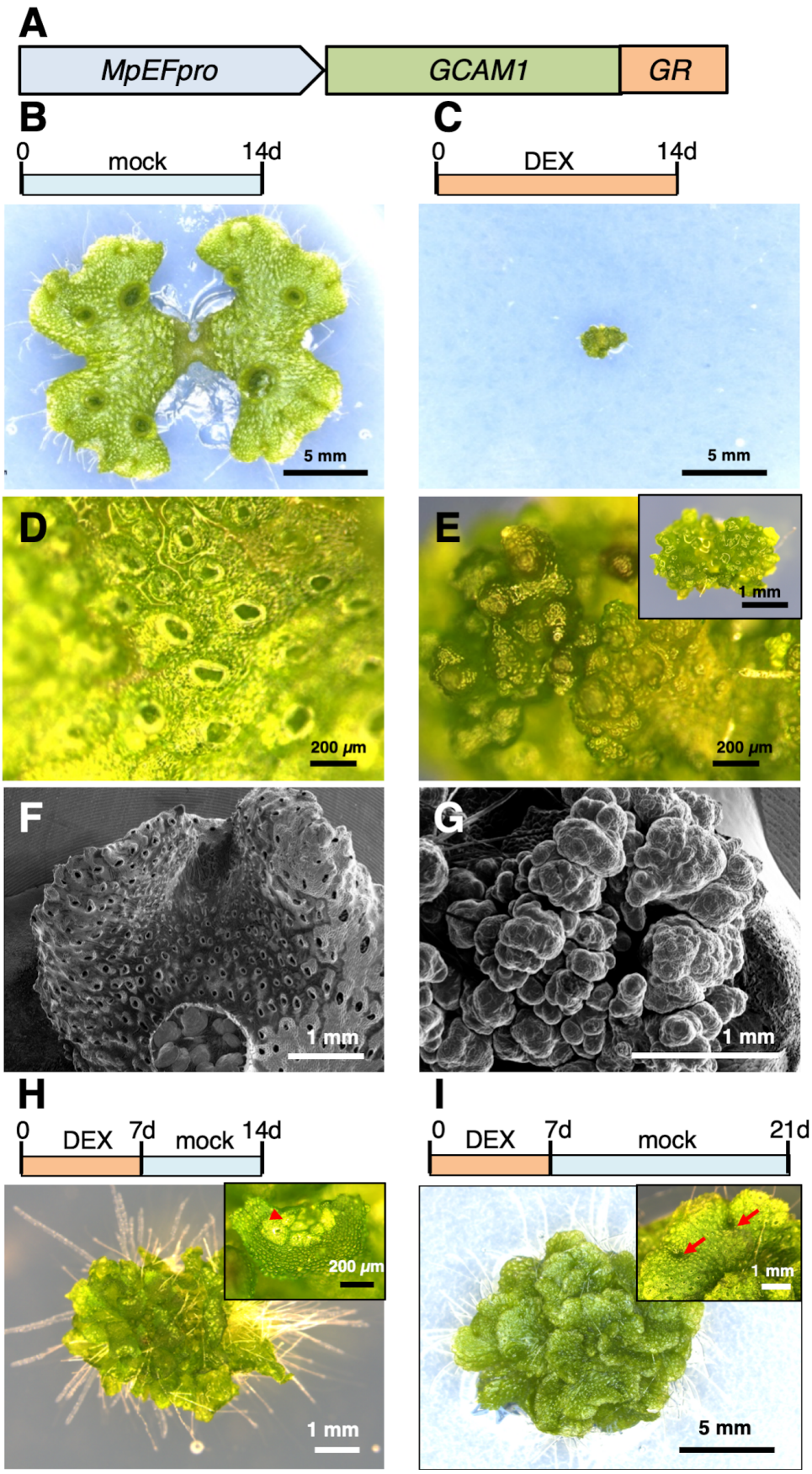

Figure 4. Yasui et al.

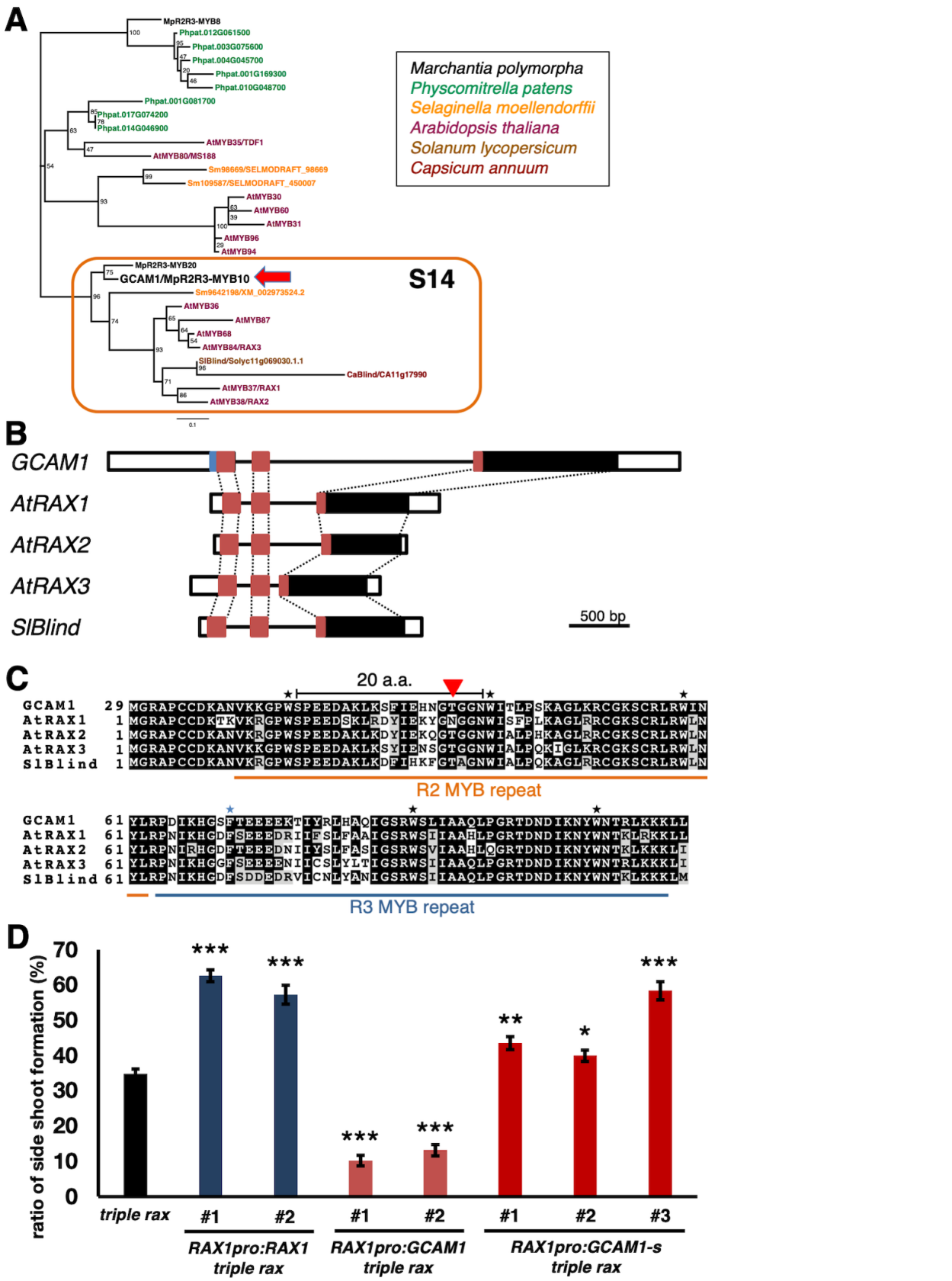

Figure 5. Yasui et al.

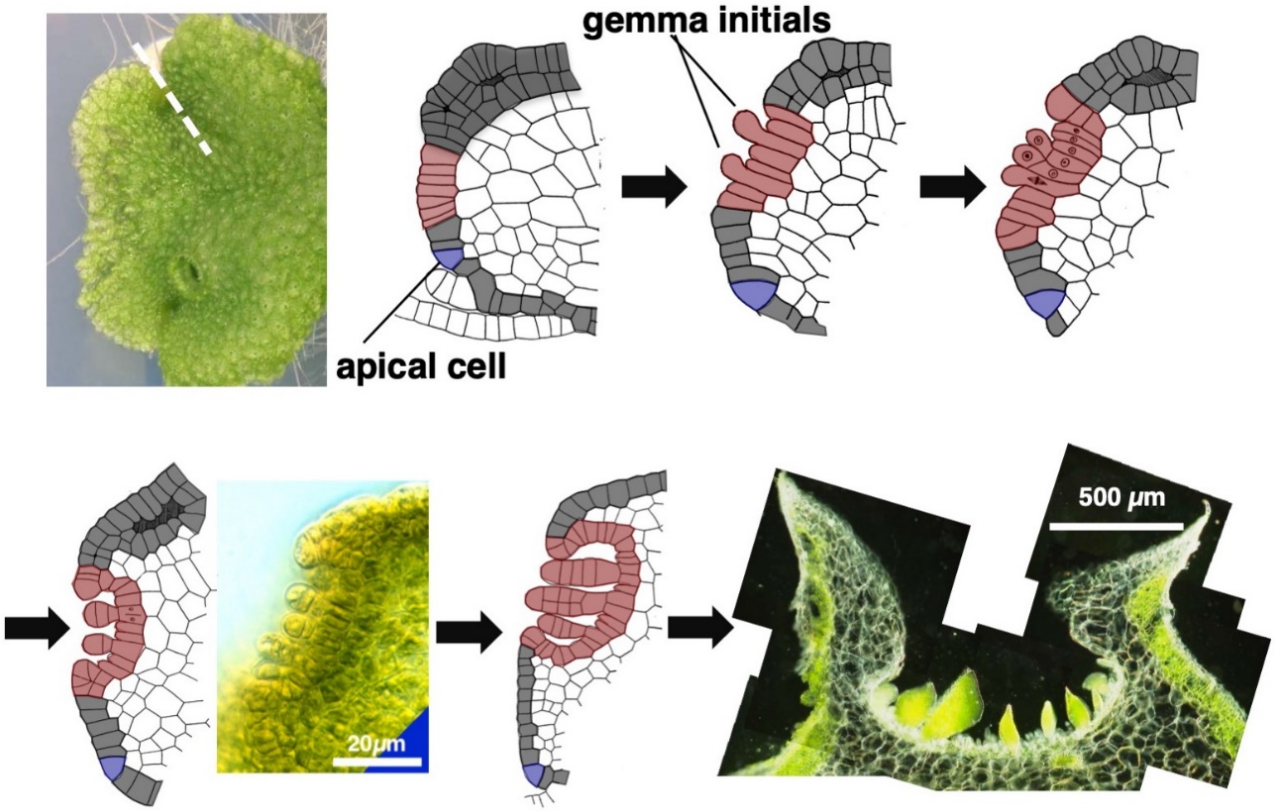

Figure S1. Histological description of the origin and development of the gemma cup in *Marchantia polymorpha*. Related to Figure 1.

Schematic representation of the early stages of gemma cup development. Illustrations of thallus sections are adapted from Barnes and Land (1908) [S1], and the precursors of the gemma cup and gemmae are highlighted in red. Apical cells are indicated in purple. The precursor of gemma cup formation can be recognized as the third cell up from the apical cell, where a periclinal cell division for air chamber formation is suppressed and a continuous single epidermis is observed. The single-layered epidermal cells will become the basal epidermis of the gemma cup floor, and undergo repeated anticlinal cell divisions to enlarge the area of the gemma cup floor. Some of the gemma cup floor cells begin to develop gemmae at an early stage of gemma cup development, and growth of the gemma cup occurs simultaneously with gemma development and maturation.

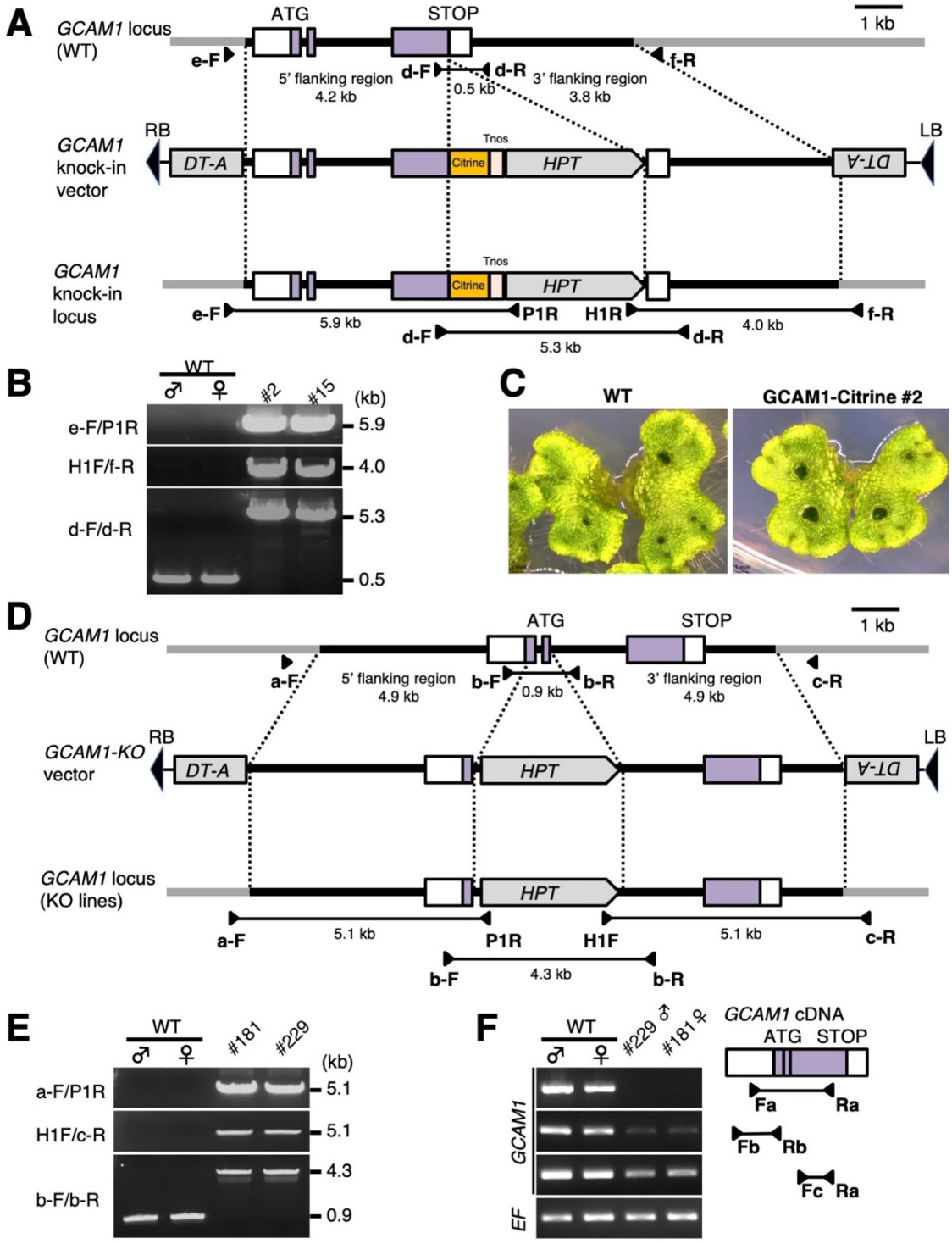

Figure S2. Generation of *GCAM1-Citrine* knock-in and *gcam1^{ko}* plants. Related to Figure 2 and 3.

(A) Structure of the *GCAM1* locus in wild-type (WT) and *GCAM1-Citrine* knock-in plants, and the knock-in vector map between the left (LB) and right (RB) borders. Black bars indicate the flanking sequences subcloned into pJHY-TMp1-Cit. Solid arrowheads indicate the positions of primers used in **(B)**. **(B)** Genomic PCR analysis of the *GCAM1* locus in WT and *GCAM1-Citrine* knock-in plants. **(C)** Mature thalli of WT and *GCAM1-Citrine* knock-in plants. No morphological abnormality was observed in *GCAM1-Citrine* knock-in plants. **(D)** Structure of the *GCAM1* locus in WT and *gcam1^{ko}* plants, and the knockout vector map between the LB and RB. Black bars indicate the flanking sequences subcloned into pJHY-TMp1, and solid arrowheads indicate the positions of primers used in **(E)**. **(E)** Genomic PCR analysis of the *GCAM1* locus in WT and *gcam1^{ko}* plants. DT-A, diphtheria toxin gene cassette; HPT, hygromycin phosphotransferase gene cassette; Tnos, nopaline synthase gene terminator sequence. White boxes indicate UTRs, and purple boxes indicates protein coding regions. **(F)** *GCAM1* mRNA expression detected by reverse-transcription PCR. Mp*EF1α* was amplified as an internal control. The number of PCR cycles was 35 (*GCAM1*) or 20 (Mp*EF1α*). Solid arrowheads indicate the primer positions in a schematic illustration of *GCAM1* cDNA.

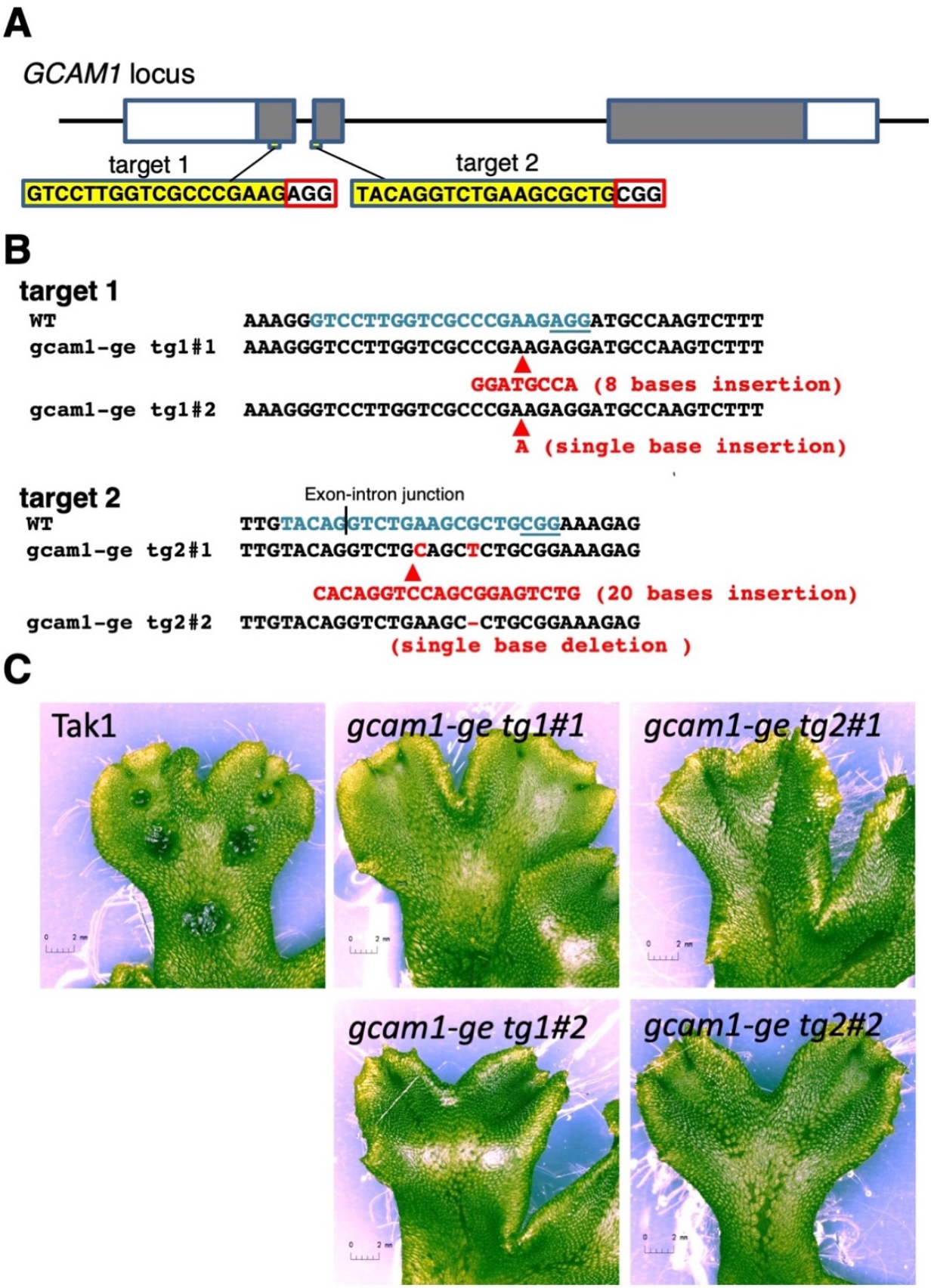

Figure S3. Targeted disruption of *GCAM1* using CRISPR/Cas9-mediated genome editing. Related to Figure 3.

(A) Schematic representation of two independent target sites in *GCAM1*. **(B)** Genome sequences of indicated target sites in wild type (WT) and targeted transgenic plants. **(C)** Upper surface of 2-week-old thallus grown from tip of thalli in WT and indicated transgenic plants.

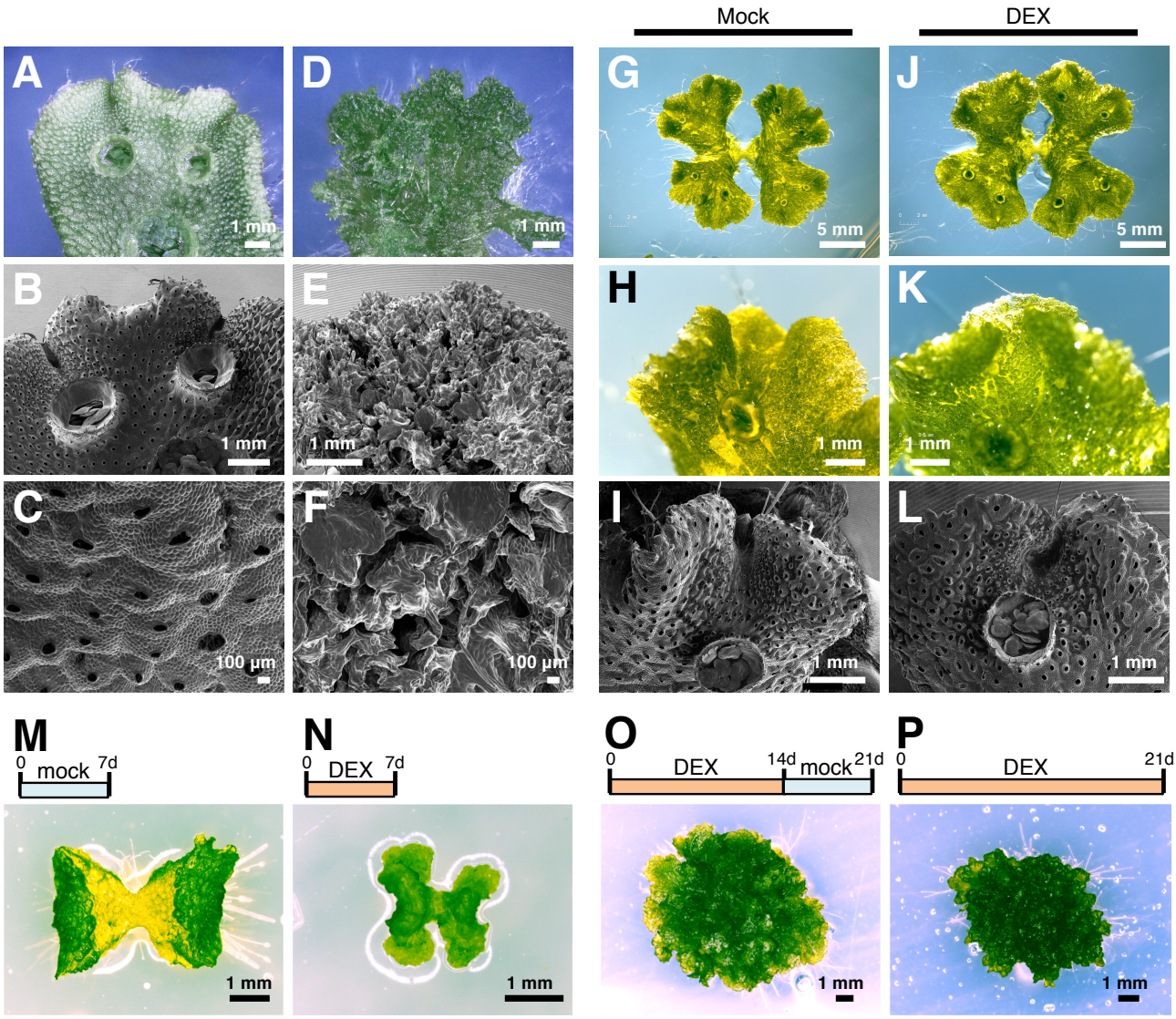

Figure S4. Overexpression of *GCAM1*. Related to Figure 4.

(A - F) 2-week-old thalli grown from tip of thalli of the wild type **(A-C)** and Mp*EFpro::GCAM1* **(D-F)** thalli. **(B, C, E, F)** Scanning electron micrographs of wild-type **(B, C)** and Mp*EFpro::GCAM1* **(E, F)** thalli. Close-up of dorsal surface of previous individual, showing numerous air pores in the wild type **(C)**, whereas no air pores were observed in the Mp*EFpro::GCAM1* **(F)** thalli.

(G - L) Effect of dexamethasone (DEX) treatment in wild type. 2-week-old thalli grown from tip of thalli of the wild type with **(J)** or without **(G)** 10 µM DEX treatment. **(H)** and **(K)** Close-up view of dorsal surface of **(G)** and **(J)**, respectively. **(L)** and **(I)**, Scanning electron micrographs of wild type thalli with **(K)** or without **(H)** 10 µM DEX treatment.

(M - P) Induction of GCAM1 function suppresses growth and organ development in thallus. **(M)** 1-week-old *MpEFpro:GCAM1-GR* transgenic plant treated with mock. (N) 2-week-old *MpEFpro:GCAM1-GR* transgenic plant treated with DEX. **(O)** 3-week-old *MpEFpro:GCAM1-GR* transgenic plant treated with DEX for the first 14 d and mock for the latter 7d. **(P)** 3-week-old *MpEFpro:GCAM1-GR* transgenic plant treated with DEX for 21d.

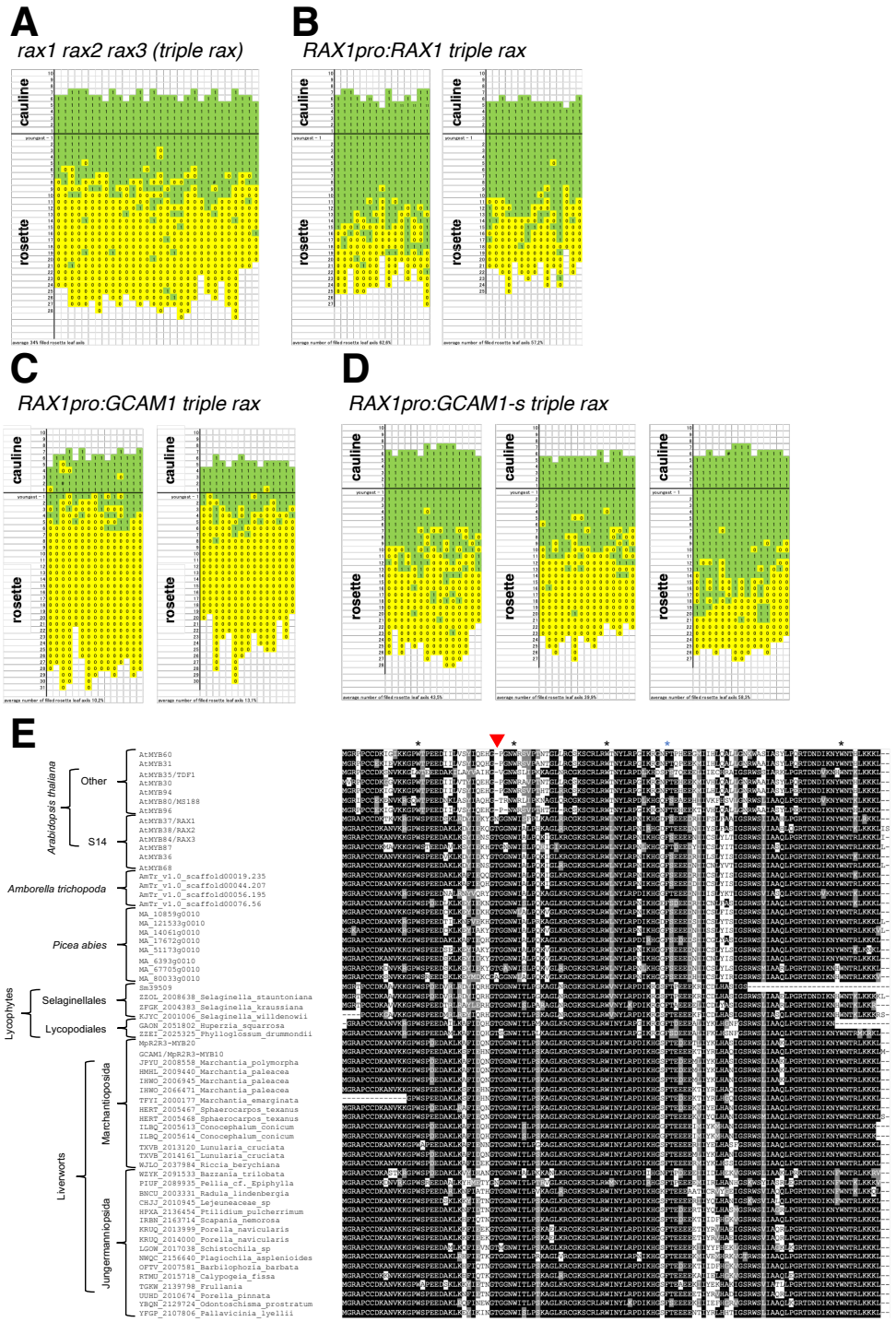

Figure S5. Interaction of GCAM1 with Arabidopsis mechanism for axillary meristem formation. Related to Figure 5.

Schematic representation of axillary bud formation in leaf axils of Arabidopsis *rax* triple mutant ($n = 30$) **(A)** transformed with *RAX1pro:RAX1* ($n = 15$ for each line) **(B)** or *RAX1pro:GCAM1* ($n = 15$ for each line) **(C)** or *RAX1pro:GCAM1-s* construct ($n = 15$ for each line) **(D)**. The horizontal line represents the border between the youngest rosette leaf and the oldest cauline leaf. Each column represents a single plant, and each square within a column represents an individual leaf axil. The bottom row represents the oldest rosette leaf axils, with progressively younger leaves above. Green indicates the presence of an axillary bud, and yellow indicates the absence of an axillary bud in any particular leaf axil. Numbers in each square indicate the number of axillary bud(s) in the axil of each leaf. Arabidopsis plants were induced to flower under long-day conditions (16 h light at 22ºC and 8 h darkness at 18ºC) after 4 weeks under short-day conditions (8 h light at 22ºC and 16 h darkness at 18 ºC). **(E)** Multiple alignment of R2R3-MYB domains of GCAM1 and related homologues in diverse lineages of land plants. Black asterisks indicate conserved Trp residues in plant R2R3-MYBs, and the blue asterisk indicates a Phe residue conserved in the R2R3-MYB subfamily 14 and some closely related subfamilies. R2R3-MYBs in subfamily 14 are characterized by an additional amino acid insertion compared with other R2R3-MYB subfamilies between the first and the second Trp residues of the R2 repeat, and the red triangle indicates the position of the insertion.

Sample name	Total reads counts	Aligned reads counts		Alignment rate (%)
		exactly once	>1 times	
Tak1; thallus 7d; rep1	18,318,924	16,558,099	621,394	90.4
Tak1; thallus 7d; rep2	18,284,886	17,102,045	544,457	93.5
Tak1; thallus 7d; rep3	19,162,536	18,006,202	569,092	94.0
Tak1; gemma-cup 21d; rep1	17,216,306	15,496,802	604,487	90.0
Tak1; gemma-cup 21d; rep2	14,489,889	13,625,766	421,670	94.0
Tak1; gemma-cup 21d; rep3	15,883,627	14,812,606	473,619	93.3
Tak1; mid-rib without gemma-cup 21d; rep1	14,774,027	13,622,665	427,230	92.2
Tak1; mid-rib without gemma-cup 21d; rep2	16,075,894	15,127,377	452,720	94.1
Tak1; mid-rib without gemma-cup 21d; rep3	15,312,864	14,337,977	474,028	93.6

Table S1. Summary of the RNA-sequencing experiment. Related to Figure 1.

Gene ID	TAIR10 BLAST tophit				RPKM value (Mean)		
	TF family	TOP hit in TAIR database	AGI code	E-value	Thallus	Mid-rib	Gemma cup
Mapoly0086s0035	B3	ABA INSENSITIVE 3 (ABI3)	AT3G24650	1E-34	8.4	6.7	25.3
Mapoly0012s0202	bHLH	RETARDED GROWTH OF EMBRYO 1 (RGE1)	AT1G49770	2E-14	4.0	1.5	14.6
Mapoly0039s0003	bHLH	RHD SIX-LIKE 1 (RSL1)	AT5G37800	4E-26	8.7	3.7	16.6
Mapoly0073s0051	bHLH	HECATE1 (HEC1)	AT5G67060	2E-20	10.1	6.4	44.2
Mapoly0126s0029	bHLH	RETARDED GROWTH OF EMBRYO 1 (RGE1)	AT1G49770	4E-28	1.9	1.0	4.0
Mapoly0072s0050	bZIP	ABSCISIC ACID RESPONSIVE ELEMENTS-BINDING FACTOR 2 (ABF2)	AT1G45249	2E-28	8.1	11.3	37.6
Mapoly0061s0011	C2H2	ZINC FINGER PROTEIN 11 (ZFP11)	AT2G42410	3E-13	2.9	1.0	9.6
Mapoly0008s0029	R2R3-MYB	AtMYB117, LATERAL ORGAN FUSION 1 (LOF1)	AT1G26780	6E-56	6.2	5.6	16.5
Mapoly0034s0034	R2R3-MYB	REGULATOR OF AXILLARY MERISTEMS3 (RAX3)	AT3G49690	3E-59	0.8	6.3	82.1
Mapoly0090s0091	MYB-related	MYB DOMAIN PROTEIN 20 (MYB20)	AT1G66230	2E-13	26.4	15.5	111.5
Mapoly0091s0012	MYB-related	MYB FAMILY TRANSCRIPTION FACTOR	AT5G41020	4E-17	0.4	0.2	2.9

Table S2. Transcription factor genes upregulated in gemma cup. Related to Figure 1.

Name	Sequence (5'→3')	Usage
GCAM1-cds-I-F	GATGTCGGGACGCAAATAAT	qRT-RCR
GCAM1-cds-I-R	TGTCATTGCGTAGGGAGATTC	qRT-RCR
GCAM1-Fa	GTAGGGAGATTCGGGGATGAA	RT-PCR
GCAM1-Ra	GGAGGTGTTGTGGTGAGAGGT	RT-PCR
GCAM1-Fb	CCTCGGCCATTACCTACAAGAG	RT-PCR
GCAM1-Rb	AAAAGGTGCGACGAGAGCA	RT-PCR
GCAM1-Fc	AATGCCGTGGGGAGAGAAG	RT-PCR
MpEF1a-F	TCACTCTGGGTGTGAAGCAG	qRT-RCR control, RT-PCR control
MpEF1a-R	GCCTCGAGTAAAGCTTCGTG	qRT-RCR control, RT-PCR control
GCAM1_ISH_probe_F	TGGTGGACGAGCATCAACAA	*in situ* RNA hybridization
GCAM1_ISH_probe_R*	tgcgtaatacgactcactatagggCGTGCGACTGGGAAGTAAGT	*in situ* RNA hybridization
MpHIS4_ISH_probe_F	GCCAAGCGTCATAGGAAGGT	*in situ* RNA hybridization
MpHIS4_ISH_probe_R*	tgcgtaatacgactcactatagggCCCGAACCCGTACAGAGTTC	*in situ* RNA hybridization
GCAM1-pro-L1	caccCTCATGTACGCAATGGTTGG	Construction of GCAM1pro:GUS
GCAM1-pro-R2	TCTGCAGCTCTTTCCGCAGCG	Construction of GCAM1pro:GUS
GCAM1-KI_5IF_L**	CCTAAGGTAGCGATTAATCGGACCCCCTGTACTGTAGAGTAC	Construction of GCAM1-Citrine knock-in construct
GCAM1-KI_5IF_R**	GGAGCCTCCAAGCTTAATACTGATCAATTTGGACAGGAAAGAATC	Construction of GCAM1-Citrine knock-in construct
GCAM1-KI_3IF_L**	TTATGTTTAAACTAGTGGGAGGAATGAAGGCCTGCTTGGTC	Construction of GCAM1-Citrine knock-in construct
GCAM1-KI_3IF_R**	TACCCTGTTATCCCTAGGTACCTTCAGACGGTTTCGCC	Construction of GCAM1-Citrine knock-in construct
d-F	GTACAACCGCTCTCAGGACCTATCT	For checking of gene targeting site for GCAM1-Citrine
d-R	GAACCCTAAGCTTTGGAGCTTGATA	For checking of gene targeting site for GCAM1-Citrine
e-F	GCCGGAACCTGAATAGAAAGAAAGAAG	For checking of gene targeting site for GCAM1-Citrine
e-R	AGATGAACTTCAGGGTCAGCTTGC	For checking of gene targeting site for GCAM1-Citrine
H1F	GTATAATGTATGCTATACGAAGTTATGTTT	For checking of gene targeting site for GCAM1-Citrine
f-R	ATGACAAGAAGAAGAAATGTCACAGTCG	For checking of gene targeting site for GCAM1-Citrine
GCAM1_5IF_L**	CTAAGGTAGCGATTAAAAGATAGGTCGCTTCGGTCAG	Construction of the targeting vector for GCAM1 knock-out
GCAM1_5IF_R**	GCCCGGGCAAGCTTAGATGGCATCCACATTCGATAAA	Construction of the targeting vector for GCAM1 knock-out
GCAM1_3IF_L**	TAAACTAGTGGCGCGTGATCACTGGGAACAAACGAAG	Construction of the targeting vector for GCAM1 knock-out
GCAM1_3IF_R**	TTATCCCTAGGCGCGTCGGTTAAAGCCTATCACACCA	Construction of the targeting vector for GCAM1 knock-out
a-F	CCTGTAATGAGTGGATTCGCTTG	For checking of gene targeting site for gcam1^{KO}
c-R	TAGGACTCGATGCTGAACTCGTC	For checking of gene targeting site for gcam1^{KO}
b-F	GCAAACCGTGAAACTCCTGTAAG	For checking of gene targeting site for gcam1^{KO}
b-R	CTTTGGAGTCTTTCCGGGTTATG	For checking of gene targeting site for gcam1^{KO}
P1R	GAAGGCTTCTGATTGAAGTTTCCTTTTCTG	For checking of gene targeting site for gcam1^{KO}
H1F	GTATAATGTATGCTATACGAAGTTATGTTT	For checking of gene targeting site for gcam1^{KO}
GCAM1_tg1-L***	gcacccagcctctcgGTCCTTGGTCGCCCGAAGgtttagagctagaa	Construction of the genome editing vector for GCAM1: target 1
GCAM1_tg1-R***	ttctagctctaaaacCTTCGGGCGACCAAGGACcgagaggctgggtgc	Construction of the genome editing vector for GCAM1: target 1
GCAM1_tg2-L***	gcacccagcctctcgTACAGGTCTGAAGCGCTGgtttagagctagaa	Construction of the genome editing vector for GCAM1: target 2
GCAM1_tg2-R***	ttctagctctaaaacCAGCGCTTCAGACCTGTAcgagaggctgggtgc	Construction of the genome editing vector for GCAM1: target 2
CRISPR-check_L	CCTGTAATGAGTGGATTCGCTTG	For checking of the edited site for GCAM1
CRISPR-check_R	TAGGACTCGATGCTGAACTCGTC	For checking of the edited site for GCAM1
GCAM1-cds-L1	caccATGCAACCTTTGCCCACTAA	Construction of entry clone containing GCAM1 coding region
GCAM1-cds-nsR	ACTGATCAATTTGGACAGGAAAGA	Construction of entry clone containing GCAM1 coding region
GCAM1-cds-sR	TTAACTGATCAATTTGGACAGGA	Construction of entry clone containing GCAM1 coding region
Myb37-pro-SbfIF	CATCCTGCAGGATAAATTAAACTATCGATTGGGTC	Introduction of GCAM1 into A. thaliana rax triple mutant
Myb37-pro-AscIR	CATGGCGCGCCTTCTCTCGTTAGTGAATTGAAGT	Introduction of GCAM1 into A. thaliana rax triple mutant
GFPAscIF	GGCGCGCCATGAGTAAAGGAGAAGAACT	Introduction of GCAM1 into A. thaliana rax triple mutant
GFPpolylinkerR	GAGCTCCCTAGGTTATTTGTATAGTTCATCCA	Introduction of GCAM1 into A. thaliana rax triple mutant
RAX1AscIF	CATGGCGCGCCATGGGAAGAGCACCGTGTTG	Introduction of GCAM1 into A. thaliana rax triple mutant
RAX1SacIR	CATGAGCTCCTAGGAGTAGAAATAGGGCA	Introduction of GCAM1 into A. thaliana rax triple mutant
GCAM1AscIF	CATGGCGCGCCATGCAACCTTTGCCCACTAA	Introduction of GCAM1 into A. thaliana rax triple mutant
GCAM1AvrIIR	CGTCCTAGGTTAACTGATCAATTTGGACA	Introduction of GCAM1 into A. thaliana rax triple mutant
GCAM1NewAscIF	CATGGCGCGCCATGGGTCGAGCTCCATGTTG	Introduction of GCAM1 into A. thaliana rax triple mutant
GCAM1AvrIIR	CGTCCTAGGTTAACTGATCAATTTGGACA	Introduction of GCAM1 into A. thaliana rax triple mutant

*Bases in lower case indicate a priming site of T7 RNA polymerase

**Underlined bases indicate the homologous sequences for cloning into pJHY-TMp1-Cit or pJHT-TMp1 using Gibson Assembly (NEB) or In-fusion cloning (TAKARA) kit.

***Bases in lower case indicate the homologous sequences for cloning into pMpGE_En01 using In-gusion cloning (TAKARA) kit.

Table S3. Oligonucleotide primers used in this study. Related to STAR Methods.

Supplemental Reference

S1. Barnes, C.R., and Land, W.J.G. (1908). Bryological papers. II. The origin of the cupule of Marchantia. Bot. Gaz. *46*, 401-409.